Stepwise progression of β-selection during T cell development as revealed by histone deacetylation inhibition

TCR co-receptors are expressed sequentially to fine-tune early αβ T cell development

[1,2]Anchi S Chann, [1,2]Mirren Charnley, [3]Lucas Newton, [2,7]Andrea Newbold, [3,4,5,6]Patrick O Humbert, [2,7]Ricky W Johnstone, [1,2,7]Sarah M Russell.

Affiliations

[1]Optical Sciences Centre, School of Science, Swinburne University of Technology, Hawthorn, Victoria 3122; Australia.

[2]Peter MacCallum Cancer Centre, Melbourne, Victoria 3000 Australia.

[3] Department of Biochemistry & Chemistry, La Trobe Institute for Molecular Science, La Trobe University, Melbourne, Victoria 3086, Australia.

[4] Research Centre for Molecular Cancer Prevention, La Trobe University, Melbourne, Victoria 3086, Australia.

[5] Department of Biochemistry & Pharmacology, University of Melbourne, Melbourne, Victoria 3010, Australia.

[6] Department of Clinical Pathology, University of Melbourne, Melbourne, Victoria 3010, Australia.

[7]Sir Peter MacCallum Department of Oncology, The University of Melbourne, Victoria 3010, Australia.

*To whom correspondence should be addressed: Sarah Russell: sarah.russell@petermac.org; 613-433-354-996; Optical Sciences Centre, School of Science, Hawthorn, Australia

ORCID ID: 0000-0002-8778-5327 (ASC); ORCID ID: 0000-0003-3845-9290 (MC); ORCID ID: 0000-0002-1366-6691(POH); 0000-0001-5826-9641 (SMR); 0000-0001-7053-9237 (RWJ); 0000-0002-0481-2431 (AN)

Abstract

During T cell development, the first step in creating a unique T Cell Receptor (TCR) is the genetic recombination of the TCRβ chain. The quality of the newly recombined TCRβ is assessed at the β-selection checkpoint. Most cells fail this checkpoint and die, but the coordination of the complex events that control fate at the β-selection checkpoint is not yet understood. We shed new light on fate determination during β-selection using a selective inhibitor of histone deacetylase 6, ACY1215. ACY1215 disrupted the β-selection checkpoint. Characterising the basis for this disruption revealed a new, pivotal stage in β-selection, bookended by upregulation of the TCR co-receptors, CD28 and CD2 respectively. Within this 'DN3b^{Pre}' stage, CD5 and Lef1 are upregulated to reflect pre-TCR signalling and their expression correlates with proliferation. During this phase, ACY1215-mediated disruption of the organisation of the β-selection immunological synapse is associated with a breakdown in connectivity of expression of pre-TCR, CD5 and Lef1. Subsequent deregulation of pre-TCR-induced proliferation leads to bypass of the β-selection checkpoint and subsequent failure to progress. We propose that the progressive expression of CD28, CD5 and Lef1, then CD2 reports and modulates the pre-TCR signal to orchestrate passage through the β-selection checkpoint. These findings suggest a refined model of β-selection in which a coordinated increase in expression of pre-TCR, CD28, CD5 and Lef1 provides for escalating TCR signalling strength, and culminates in the expression of CD2 to enable exit from the β-selection checkpoint.

Introduction

T cells are generated in a multistep, highly orchestrated process guided by stromal cells in the thymus. T cell development involves massive cell proliferation interspersed with genomic recombination of the T cell receptor (TCR). If genomic recombination, proliferation and death are not appropriately orchestrated, the implications for cancer and immunity are profound. Uncontrolled self-renewal or a sub-optimal TCR repertoire can lead to T cell acute lymphoblastic lymphoma (T-ALL), autoimmunity or limited response to pathogens or cancers (Ballesteros-Arias et al., 2019; Douek et al., 2000; Notarangelo et al., 2020). T cell development is most tightly controlled during genomic recombination to generate the TCR. For the most common αβ T cells, the β chain is generated at the

58 DN3a phase of T cell development (see **Supp Fig 1A** for a description of T cell development and the
59 surface markers by which it is assessed), and the appropriateness of this TCRβ sequence is assessed
60 during the β-selection checkpoint. During β-selection, the strength of the TCRβ chain is tested in
61 combination with a surrogate 'pre-TCR' before the TCRα chain is created (Chann and Russell, 2019;
62 Dutta et al., 2021).

63 β-selection is in part determined by stromal cells in the thymic microenvironment, which provide
64 Notch and chemokine signals that promote survival and differentiation (Chann and Russell, 2019;
65 Dutta et al., 2021). Recently, it has become clear that interactions between the pre-TCR and the
66 MHC-peptide on stromal cells also provide an opportunity to test TCR signalling (Allam et al., 2021;
67 Dutta et al., 2021; Li et al., 2021) These interactions trigger a sequence of transcriptional changes and
68 epigenetic modifications that ensure only the cells with an appropriately recombined TCRβ chain
69 survive, proliferate and differentiate. How pre-TCR signalling integrates fate determination including
70 proliferation, differentiation and survival during β-selection is still not understood (Chann and
71 Russell, 2019; Dutta et al., 2021).

72 Epigenetic therapies such as small-molecule inhibitors of histone deacetylases (HDAC) have shown
73 great promise in mediating clinical antitumor responses and are emerging as immune modulators
74 (Hogg et al., 2020). The HDAC6 selective inhibitor ACY1215 (Ricolinostat) can synergize with the
75 BET inhibitor, JQ1, to recruit T cell mediated responses to lung adenocarcinoma, enhance T cell
76 responses to *ex vivo* melanoma cultures, impair effector CD8 T cell function during skin
77 inflammation, and alter Treg function (Adeegbe et al., 2017; Laino et al., 2019; Tsuji et al., 2015; Xu
78 et al., 2018; Zhang et al., 2021). HDACs 1, 2, and 3 are required at multiple stages of T cell
79 development, but a role for HDAC6 in T cell development has not been identified (Wang et al., 2020).
80 Mice lacking HDAC6 showed no overt T cell phenotypes (Shapiro and Shapiro, 2020; Zhang et al.,
81 2008) and to our knowledge the effect of acute deletion of HDAC6, or pharmacological inhibition of
82 HDAC6 on T cell development has not been reported (Shapiro and Shapiro, 2020). Here, we show a
83 striking effect of treatment with the HDAC6-selective inhibitor, ACY1215, on β-selection.

84 This effect of ACY1215 allowed us to define several stages of β-selection with high resolution. After
85 the DN3a stage marked by upregulation of the co-receptor, CD28, we observed a transitional stage
86 marked by low levels of the co-receptor, CD2, that we termed DN3b^{Pre}. DN3b^{Pre} cells are enriched by
87 ACY1215 treatment. An upregulation of CD2 marks passage through the β-selection checkpoint, to a
88 phase we termed DN3b^{Post}. The transcription factor, Lef1 is upregulated in DN3b^{Pre} cells, together
89 with an increasing expression of the reporter of TCR signalling, CD5. These findings implicate a
90 refined model of β-selection in which, following expression of CD27 and CD28, a coordinated
91 increase in expression of pre-TCR, CD5 and Lef1 provides for an escalating test of TCR signalling.
92 Expression of CD2 marks the passing of this test and exit from the β-selection checkpoint.

93

94 **Results**

95 **Treatment with ACY1215 impairs T cell differentiation at the β-selection stage.**

96 To examine the effects of ACY1215 on T cell development, we used two models. Firstly, a well
97 validated *in vitro* model in which hematopoietic stem cells extracted from mouse fetal liver were co-
98 cultured with the OP9 mouse bone marrow stromal cell line transfected with the Notch ligand, DL1
99 ('OP9-DL1') (Holmes and Zúñiga-Pflücker, 2009). To assess relevance of our findings to
100 physiological T cell development in the thymus, we also analysed cells directly taken from young
101 adult mice.

102 At Day 8-10 of the co-culture, when cells from mouse fetal liver were predominantly at the DN3 stage
103 of T cell development **(Supp Fig 1B**), we applied the HDAC6 inhibitor, ACY1215 at a concentration
104 previously reported to alter function of mature T cells without affecting lymphocyte viability (Laino
105 et al., 2019). Compared with DMSO-treated cells, cells treated with ACY1215 for two days (**Figure**
106 **1A**) showed reduced proportions of the later stages of differentiation, suggesting HDAC6 is required
107 for optimal T cell development to the DP stage. This shift in differentiation was accompanied by a
108 generalised inhibition of expansion in cell numbers at several stages of T cell development (**Supp Fig**
109 **2A**). Comparing proportions at different DN stages using CD25 and CD44 expression (Figure 1A)

110 showed an increase in the proportions of DN3 cells and commensurate decrease in proportions of
111 DN4, suggesting that the ACY1215-treated cells were blocked at the DN3 stage.

112 The DN3 stage incorporates the β-selection checkpoint. The passing of the β-selection checkpoint,
113 conventionally conceptualised as DN3a-to-DN3b progression, is marked by the expression of CD28
114 (Teague et al., 2010; Williams et al., 2005). Therefore, we assessed whether DN3a (DN3, $CD28^{Lo}$)
115 cells were inhibited from progressing to DN3b (DN3, $CD28^{Hi}$) by ACY1215 treatment over one and
116 two days (**Figure 1B**). Surprisingly, the reverse was observed. Co-staining with CD25 and CD28
117 indicated a relatively stable distribution between DN3a and DN3b at 1 and 2 days in the control
118 cultures, but increasingly greater proportions of DN3b cells in the ACY1215-treated cultures. A
119 similar shift to DN3b and DN4 at the expense of DN3a was observed in thymocytes extracted from an
120 adult mouse and cultured for 1 day on OP9-DL1, although the relatively low numbers of DN3a in
121 primary thymocytes *ex vivo* made the shift less obvious (**Figure 1C, Supp Fig 1C**).

122 We explored the cellular basis of this shift away from DN3a towards DN3b. Cell counts of cultures of
123 sorted DN3a cells showed that the DN3a cells expanded more than 4-fold over 2 days of control
124 DMSO-treated culture, but this was dramatically reduced by ACY1215 treatment (Fig 1B**)**. In
125 contrast, ACY1215 caused a negligible reduction in absolute numbers of DN3b and DN4 cells arising
126 from DN3a. This stage-specific effect was probably not due to differences in proliferation or death
127 because CFSE and Ki-67 labelling showed similar inhibition of proliferation of DN3a and DN3b cells
128 (**Supp Fig 3**) and neither DN3a or DN3b cells were demonstrably susceptible to cell death, although
129 DP cells died more in the presence of ACY1215 (**Supp Fig 4**). Together, these data suggest that
130 ACY1215 treatment of DN3a cells led to reduced amplification, but little impact or a compensatory
131 increase in the number of cells passing through the DN3b stage.

132 To reconcile the seemingly normal progression through β-selection (as indicated by DN3b and DN4
133 counts) with the block in DP cells, we first monitored differentiation from sorted DN3a and DN3b
134 cells that had been treated for four days with ACY1215 or DMSO (**Supp Fig 5**). Progression past the
135 DN3 stages was inhibited for both DN3a and DN3b starting populations, although less clear for the
136 DN3a starting population due to limited differentiation by Day 4. To confirm that the effect at β-

137 selection led to a downstream impact on DP cells, we counted the number of cells at each
138 differentiation stage that developed from the sorted DN3b population (**Figure 1D**). By day 4, DN3b
139 cells had expanded more than 50-fold, with a negligible reduction caused by treatment with
140 ACY1215. DN4 cell numbers were also only slightly reduced by ACY1215 treatment, but DP were
141 reduced by over two orders of magnitude. These data together suggest that ACY1215 treatment
142 impacts generally upon cell expansion, but also alters differentiation to DP by acting at the DN3
143 stage, perhaps by causing precocious differentiation from DN3a to DN3b.

144 The DN3 cell stage involves fate choice between two T cell lineages (αβ cells and γδ cells), each
145 expressing a different set of T cell receptors (Hayday and Pennington, 2007). To determine which
146 lineage was altered by ACY1215, we cultured developing T cells for 2 days with and without
147 HDAC6i and labelled the cells with antibodies specific for these TCRs to assess progression through
148 the DN and DP stages (**Supp Fig 6**). ACY1215 treatment reduced the proportion of TCRβ–expressing
149 cells at all stages following β-selection but did not inhibit TCRγδ development. Together, these data
150 indicated that the defect in differentiation to DP following ACY1215 treatment was specific to αβ T
151 cells, and likely involved the β-selection checkpoint.

152 One possible explanation for this passage to DN3b without optimal subsequent differentiation could
153 be that ACY1215-treated cells express some markers suggestive of differentiation, but are not
154 competent precursors of αβ T cells. To assess this, we first characterised several phenotypic markers
155 implicated in progression through the β-selection checkpoint. Co-staining DN3 cells with both CD28
156 and CD27, both of which can discriminate between DN3a and DN3b cells (Taghon et al., 2006;
157 Teague et al., 2010) clearly discriminated two subpopulations in DN3 cells pre-treated with DMSO
158 (**Figure 2A**). A shift from DN3a to DN3b is observed for both fetal liver-derived lymphocytes and *ex*
159 *vivo* extracted thymocytes cultured on OP9-DL1 stroma. These data confirm the findings above that,
160 at least by the canonical markers, CD27 and CD28, ACY1215 treatment promotes differentiation
161 towards DN3b at the expense of DN3a.

162 Given that the primary function of this checkpoint is to ensure appropriate TCRβ rearrangement, we
163 assessed the correlation of each marker with TCRβ expression (**Figure 2B**). As previously shown

164 (Williams et al., 2005), expression of CD28 was clearly correlated with expression of icTCRβ in cells
165 derived from fetal liver or from the adult thymus. The $CD28^{Hi}$ cells also expressed more of the
166 nutrient transporters, CD71 and CD98, and more surface TCRβ (**Supp Fig 7A**) indicating that, in
167 general, they had progressed further through β-selection, but the correlation was not absolute. For
168 both cell sources, ACY1215 treatment resulted in less icTCRβ expression in the DN3b (whether
169 measured as $CD28^{Hi}$ or $CD27^{Hi}$ DN3 cells) (Fig 2B, see also Supp Fig 8C). To validate the icTCRβ
170 staining, we directly compared it with surface TCRβ (**Supp Fig 7B**). For both cell sources, expression
171 of surface TCRβ was highly correlated with that of icTCRβ and both were reduced by ACY1215
172 treatment. Thus, as well as depleting DN3a cells, treatment with ACY1215 increases the proportions
173 of a cell population that bears many of the phenotypic markers of passage through β-selection, but
174 these cells appear somewhat defective in expression of TCRβ, and do not progress optimally through
175 the DP stage. We speculated that further characterisation of these cells might yield valuable
176 information about requirements at the β-selection checkpoint.

177 **CD2 expression identifies $DN3b^{Pre}$ and $DN3b^{Post}$ as two functionally distinct stages in β-selection.**

178 A well-established co-stimulator of TCR signalling is CD2 (Skånland et al., 2014). Expression of
179 CD2 marks TCRβ V(D)J rearrangement and can facilitate pre-TCR signalling for passage through the
180 β-selection checkpoint (Groettrup et al., 1992; Rodewald et al., 1993; Sasada and Reinherz, 2001). In
181 the next series of experiments, we find that CD28 and CD2 reliably define 3 sequential stages of β
182 selection in DN3 cells, which we term DN3a, $DN3b^{Pre}$, and $DN3b^{Pro}$ to accommodate pre-existing
183 nomenclature (**Figure 3A**). Co-staining of DMSO-treated DN3 cells with CD28 and CD2 showed that
184 all DN3a cells ($CD28^{Lo}$) were $CD2^{Lo}$, but DN3b ($CD28^{Hi}$) cells had two clearly discernible
185 populations of $CD2^{Lo}$ ($DN3b^{Pre}$) and $CD2^{Hi}$ ($DN3b^{Pro}$) (**Figure 3Bi**). ACY1215 treatment enriched for
186 the $DN3b^{Pre}$. Cell counts indicated that the numbers of $DN3b^{Pre}$ cells were not substantially affected
187 by ACY1215, but DN3a and $DN3b^{Post}$ numbers were dramatically reduced (**Supp Fig 8A**). Thus,
188 ACY1215 treatment led to an enrichment in a $DN3b^{Pre}$ population that was low for CD2. The $DN3b^{Pre}$
189 population **(Fig 3Bii)** was evident in thymocytes from young adult mice, even without *in vitro* culture
190 (see Fig 4 below), and was again enriched by treatment with ACY1215.

191 To confirm that DN3b^{Pre} cells were earlier in β-selection than DN3b^{Post} cells, we assessed the
192 association of CD2 expression with proliferation as measured by CFSE dilution (**Supp Fig 8B**). Two
193 clear populations were evident, with the CD2^{Hi} (DN3b^{Post}) cells having undergone substantially more
194 proliferation than the CD2^{Lo} (DN3b^{Pre}) cells. ACY1215 treatment did not disrupt the association
195 between CD2 and proliferation. Expression of CD27 and surface TCRβ were also increased from
196 DN3a, DN3b^{Pre}, to DN3b^{Post}, with stepwise correlation which was not altered by ACY1215 despite
197 lower surface TCRβ on DN3b^{Post} cells (**Supp Fig 8C**). We then assessed icTCRβ and Ki-67 staining,
198 which should reflect the cell proliferation triggered by successful passage through the β-selection
199 checkpoint (**Figure 3C**). Indeed, consistent with previous findings that TCRβ V(D)J recombination is
200 restricted to DN cells positive for CD2 (Rodewald et al., 1993), DN3b^{Pre} cells were intermediate in
201 expression of icTCRβ and Ki67i.e. between the levels seen on DN3a cells and DN3b^{Post} cells. The
202 correlated, stepwise increase in icTCRβ and Ki-67 was observed in cultures from both fetal liver and
203 adult thymus (Figure 3Ci & ii). This pattern was even more striking in thymocytes from adult mice,
204 where DN3a cells showed no proliferation, DN3b^{Pre} cells were heterogeneous with respect to
205 proliferation, and proliferation correlated with icTCRβ expression, and DN3b^{Post} cells were all highly
206 proliferative, with minimal impact from ACY1215 treatment. These data suggest that the dramatic
207 reduction in TCRβ expression upon ACY1215 treatment observed in Fig 2 was explained more by the
208 enrichment of DN3b^{Pre} cells, by than a direct effect on TCRβ expression. c-Myc, which mediates the
209 proliferative response to pre-TCR signalling but is not required for differentiation (Dose et al., 2006),
210 showed a similar stepwise increase with these differentiation stages (**Supp Fig 8D**). These data are all
211 compatible with an interim DN3b^{Pre} stage that reflects an early, and pivotal step in β-selection where
212 rearrangement of the TCRβ chain is translated into proliferation.

213 To formally assess whether the DN3b^{Pre} stage is a transitional stage before DN3b^{Post}, we sorted DN3a,
214 DN3b^{Pre} and DN3b^{Post} cells from adult mice and cultured them for further analysis (**Figure 4**).
215 Analysis of the cells immediately after extraction showed clearly distinct DN3a, DN3b^{Pre} and
216 DN3b^{Post} cells. After two days, DN3b^{Post} cells had produced substantial numbers of DP cells, with
217 fewer produced by DN3b^{Pre}, and fewer still by DN3a cells. Also compatible with unidirectional

218 progression from DN3a to DN3b^{Pre} to DN3b^{Post}, was the proportion of DN4 and DN3 stages from each
219 sorted population. ACY1215 treatment of thymocytes stabilized the DN3b^{Pre} population and blocked
220 progression to DP. Similar data was obtained in the fetal liver-derived cultures (**Supp Fig 9**). These
221 data confirm that DN3b^{Pre} (CD28^{Lo}CD2^{Lo}) is a transitional state between DN3a (CD28^{Hi}CD2^{Lo}) and
222 DN3b^{Post} (CD28^{Hi}CD2^{Hi}), reflecting partial progression through β-selection.

223 **ACY1215 alters the pre-TCR signalling platform clustered at MTOC**

224 The enrichment of CD28^{Hi}CD2^{Lo} DN3b^{Pre} cells by ACY1215 treatment in both fetal liver-derived
225 cells and thymocytes from adult mice suggests that a key process in this stage might involve
226 acetylation. We explored three possible mechanisms by which ACY1215 might disrupt β-selection.
227 ACY1215 is selective for HDAC6, and can inhibit the catalytic activity of HDAC6 (Eich et al., 2018;
228 Narita et al., 2019). HDAC6 protein is expressed at every stage of T cell development (**Supp Fig**
229 **10A**). The best-known role of HDAC6 is in modification of histones for epigenetic regulation. Indeed,
230 acetylation of H3K18 was increased upon treatment with ACY1215, suggesting that epigenetic
231 modification could be affected by the drug (**Supp Fig 10B**). Although best known as a regulator of
232 histone acetylation, HDAC6 can also acetylate α-tubulin (Narita et al., 2019). In mature T cells, the
233 regulation of acetylation of α-tubulin by HDAC6 influences TCR-mediated recruitment of the
234 microtubule-organising centre (MTOC) to the immunological synapse (Serrador et al., 2004). In all T
235 cell developmental stages, HDAC6 was predominantly in the nucleus, but also detectable in the
236 cytoplasm and near the MTOC, compatible with effects on MTOC modification (**Supp Fig 10C-E**).
237 Acetylation of α-tubulin (K40), which can be de-acetylated by HDAC6 (Osseni et al., 2020), was
238 evident throughout the T cell differentiation stages (**Figure 5A**). Upon a two-hour treatment with
239 ACY1215, each population showed an increase in acetylated tubulin, suggesting HDAC6 deacetylated
240 tubulin throughout early T cell development.

241 We previously found that T cells undergoing β-selection form an immunological synapse, in which
242 MTOC and other TCR-associated signalling proteins move with the MTOC to the site of antigen
243 receptor signalling receptor signalling (Allam et al., 2021). We therefore speculated that an alteration
244 in MTOC organisation might mediate the effects of ACY1215 on β-selection by impacting the

245 immunological synapse. To address this, we first assessed the association of LAT with the MTOC in
246 DN3a cells (**Figure 5B**). Acetyl-α-tubulin presented as a single cluster in the site of the MTOC, and
247 was increased in intensity with ACY1215 treatment, compatible with the flow cytometry results.
248 LAT was strongly associated with the MTOC in DMSO treated cells, but altered by ACY1215
249 treatment, with less intense fluorescence and less clustering at the MTOC. Notch is particularly
250 important during β-selection in mediating assembly of the immunological synapse and transmitting
251 signals downstream of the pre-TCR signal (Allam et al., 2021; Charnley et al., 2020). We therefore
252 assessed the co-localisation of Notch1 and the MTOC in DN3a cells (**Figure 5C**). In DMSO treated
253 cells, Notch was concentrated at the MTOC, but, similar to LAT, was much more diffuse following
254 ACY1215 treatment. Interestingly, the change in localisation of both Notch and LAT was
255 accompanied by a loss in their intensity. A reduction in surface Notch expression was observed in
256 DN3a, DN3b and DN4 cells, suggesting that the reduction in Notch1 transcription that normally
257 occurs following β-selection (Yashiro-Ohtani et al., 2009) might be accelerated by ACY1215 (**Fig**
258 **5D**). Together, these data suggest that a possible mechanistic basis for the effects of ACY1215 on β-
259 selection is via alterations in recruitment by MTOC of Notch1 and TCR signalling components to the
260 immunological synapse, associated with enhanced tubulin acetylation at the immunological synapse.

261 **DN3b^{Pre} cells have commenced but not completed β-selection, and are controlled by sequential**
262 **changes in key regulators of β-selection.**

263 How might such a disruption in the immunological synapse and TCR signalling alter progression
264 from DN3b^{Pre} to DN3b^{Post}? A collaboration between pre-TCR and Wnt signalling is well established,
265 with two core Wnt pathway transcriptional regulators: β-catenin and Lef1/TCF-1 essential to β-
266 selection (Gounari et al., 2001; López-Rodríguez et al., 2015; Staal and Clevers, 2005; Travis et al.,
267 1991; Xu et al., 2009; Zhao et al., 2021). TCF-1 and Lef1 can directly modify histone acetylation, and
268 this function is inhibited by the pharmacological HDAC inhibitors, Tubacin and Vorinostat, (Xing et
269 al., 2016; Zhao et al., 2021). In support of functional interplay between ACY1215 treatment and TCF-
270 1 and Lef1, TCF-1 deficiency leads to a similar phenotype as ACY1215 treatment, with disrupted β-
271 selection and reduced expression of icTCRβ in DN4 cells (Goux et al., 2005), and deletion of both

272 TCF-1 and Lef1 leads to a complete block at DN4 (Yu et al., 2012). We focused on Lef1 since Lef1 is
273 specifically expressed at the β-selection stage (Mingueneau et al., 2013). To assess whether Lef1
274 might mediate the β-selection decisions at the DN3b^{Pre} stage, we explored how its expression changed
275 with differentiation, and how it was impacted by ACY1215 treatment. Lef1 was minimally expressed
276 in DN3a cells, uniformly bright in DN3b^{Pro} cells, but heterogeneous in DN3b^{Pre} cells derived from
277 either fetal liver or adult thymus (**Fig 6Ai & ii**). In the DN3b^{Pre} cells, Lef1-expression was associated
278 with increased expression of TCRβ, albeit with a wide range in TCRβ expression (**Fig 6B**). ACY1215
279 treatment did not demonstrably alter icTCRβ expression (Fig 6B) but, prevented the upregulation of
280 Lef1 expression in DN3b^{Pre} cells, suggesting a role in pre-TCR-mediated induction of Lef1.

281 The correlation in expression of TCRβ with proliferation and Lef1 expression raised the possibility
282 that the pre-TCR signal might be directly translated into phenotype during the DN3b^{Pre} stage. To
283 explore this, we investigated the TCR-associated receptor, CD5. A role for CD5 has not been
284 demonstrated during β-selection, but during positive selection expression of CD5 reports the strength
285 of TCR signalling and tunes TCR signalling responsiveness, dampening the response of cells to TCR-
286 signalling via the NF-κB pathway (Azzam et al., 2001; Azzam et al., 1998; Tarakhovsky et al., 1995;
287 Voisinne et al., 2018). To explore the dynamics of CD5 expression during β-selection, we stained
288 fetal liver-derived DN3 cells with CD2, Lef1 and CD5 (**Supp Fig 11**). Gating for DN3b^{Pre} with low
289 and high Lef1 expression showed strong correlation of CD5 and Lef1expression. Interestingly, Lef1
290 upregulation was retained in the presence of ACY1215, but the correlation with CD5 expression was
291 lost. These data suggest a model in which CD5 expression is downstream of Lef1, and suggest the
292 effects of ACY1215 on progression through β-selection might be mediated by disrupting the
293 functional connection between Lef1 and CD5. Lef1 and CD5 expression were similarly correlated in
294 DN3 cells extracted from the adult thymus, particularly in DN3b^{Pre} cells (**Figure 7A**).

295 To confirm this model, we made use of the fact that progression past DN3 is marked by
296 downregulation of CD25, and a transitional stage between DN3b and DN4 (sometimes termed DN3c)
297 can be identified within the DN3 population (Ananias et al., 2008; Teague et al., 2010). We therefore
298 assessed the relationship between CD2 and CD25 in the DN3b cells. DN3b^{Pre} population was still

299 high for CD25, but DN3b^{post} included CD25^{Lo} cells. (**Supp Fig 12A**). These data are compatible with
300 the notion that DN3b^{Post} marks a later stage in differentiation, that includes, but is not exclusive to, the
301 DN3c population (Ananias et al., 2008). To assess whether the combined expression of CD5 and Lef1
302 in DN3b cells indicated progression through β-selection, we gated for the two clearly discriminated
303 sub-populations Lef1^{Lo}CD5^{Lo} and Lef1^{Hi}CD5^{Hi}, and compared their CD25 expression (**Supp Fig**
304 **12B**). The Lef1^{Hi}CD5^{Hi} cells were substantially lower for CD25, indicating that they had already
305 progressed through β-selection. Although as expected there were far fewer cells in the Lef1^{Hi}CD5^{Hi}
306 population upon ACY1215 treatment, they also exhibited the reduction in CD25, suggesting that
307 ACY1215-treated cells can precociously differentiate beyond β-selection in the absence of CD5
308 expression.

309 To confirm the relationship between pre-TCR and CD5 and to assess the impact of ACY121, we
310 cultured DN3a or DN3b cells from adult thymus in the presence of ACY1215 or DMSO for 2 days,
311 gated for DN3b cells, and compared CD5 expression to icTCRβ (**Figure 7B**). Cells from the DN3a
312 starting population were more likely to be dull for both CD5 and icTCRβ, compared with the more
313 mature cells from the DN3b starting population. However, in these mature cells, expression of
314 icTCRβ correlated with expression of CD5, suggesting that, as in other cell types, CD5 expression
315 might report TCR signalling strength during β-selection. In ACY1215-treated cells, expression of
316 surface TCRβ was reduced by the DN3b^{Post} stage, and uncoupled from CD5. Similar findings were
317 obtained using fetal liver cultures and staining for CD5 and icTCRβ (**Supp Fig 13**). The correlation of
318 TCRβ with CD5, and its uncoupling after ACY1215 treatment, was not observed with CD27 and
319 CD28 (Figure 2) nor CD2 (Fig 3). Together, a functional link between pre-TCR, Lef1and CD5 is
320 coordinated at DN3b^{Pre} stage (**Figure 7C**), and is affected by ACY1215.

321 To assess the functional relationship between TCRβ and CD5, we compared CD5 expression and
322 proliferation in the presence and absence of ACY1215 (**Figure 8A**). Proliferation was minimal in
323 most DN3a cells and DN3b^{Pre} cells, but was evident in a portion of DN3b^{Pre}, cells from the DN3b
324 starting population, and in DN3b^{Post} cells. This proliferation was clearly correlated with CD5
325 expression in control cells. However, the correlation between CD5 expression and CFSE dilution was

326 lost in the DN3b^{Pre} cells that had been treated with ACY1215. These data together indicate that CD5
327 serves as a link between TCRβ expression and proliferation, and that this link is broken by ACY1215
328 treatment.

329

330 **Discussion**

331 A critical factor in β-selection is the sequential expression of specific transcriptional regulators, with
332 differential perdurance and cross-inhibition ensuring checks and balances that prevent inappropriate
333 survival and differentiation (Chann and Russell, 2019; Zhao et al., 2021). Many such checks and
334 balances have been identified to play important roles during β-selection, but the stepwise progression
335 of events that dictate fate have been elusive (Chann and Russell, 2019; Zhao et al., 2021). Our
336 explorations into effects of an HDAC6 inhibitor have revealed sa new working model (**Figure 8C,**
337 **Supp Fig 14**), Once DN3b^{Pre} cells have entered the β-selection checkpoint, they respond to graded
338 levels of TCRβ by expressing Lef1, then CD5. Normally, proliferation only occurs in cells expressing
339 CD5. Passing of the β-selection checkpoint is then marked by the expression of CD2. The disruption
340 in TCRβ-associated expression of CD5 by ACY1215 provides a possible mechanism for the escape of
341 cells lacking an appropriately rearranged TCRβ chain following ACY1215 treatment, although such a
342 role remains to be investigated.

343 The upregulation of CD27 and CD28 is gradual, but the upregulation of CD2 is more abrupt, making
344 for a convenient demarcation of differentiation stages. Our findings are compatible with previous
345 observations that CD2 expression marks cells with TCRβ gene rearrangement (Rodewald et al.,
346 1993), that knockout of CD2 inhibits progression to the DN4 stage but does not influence TCRβ
347 repertoire (Sasada and Reinherz, 2001), and suggestions of cis-regulation of CD2 and TCRβ
348 expression involving chromatin structure (Kamoun et al., 1995) Together, these findings suggest that
349 expression of CD2 (marking entrance to the DN3b^{Post} stage) reflects a completion of TCRβ
350 recombination and triggers critical fate-determining events that involve progressive upregulation of

351 CD5 and Lef1. CD2 in mature T cells sets quantitative thresholds for activation (Bachmann et al.,
352 1999), suggesting the possibility that a similar process could be involved in β-selection.

353 **Ideas and Speculation**

354 A novel finding from this work is that CD5 levels are modified in association with pre-TCR
355 expression, and that treatment with ACY1215 prevents the upregulation of CD5 (but has a lesser
356 effect on Lef1 upregulation) during β-selection. At other stages of T cell development and activation,
357 CD5 reports on the strength of TCR signalling, with increasing expression reflecting a stronger TCR
358 signal (Azzam et al., 1998; Sood et al., 2021; Tarakhovsky et al., 1995). Our findings that the
359 correlation of CD5 with TCRβ expression is lost with ACY1215 treatment, but the correlation of CD5
360 expression with proliferation is retained with ACY1215 treatment, suggest the possibility that CD5
361 plays a similar role as a reporter of pre-TCR signalling. Interestingly, it is now emerging that
362 differential CD5 expression also marks the propensity for different fates in thymocytes and $CD4^+$ T
363 cells, and this reflects transcriptional and epigenetic differences between cells with high and low CD5
364 expression (Rogers et al., 2021). In other cell types the combined action of responding to, and
365 dampening, the TCR signal, allows CD5 to tune the TCR signal and so shift the window and modify
366 the timing of positive selection (Lutes et al., 2021; Matson et al., 2020; Sood et al., 2021; Voisinne et
367 al., 2018). Whether or not such a tuning role might occur for CD5 during β-selection needs further
368 exploration, but a possible role for tuning of the TCRβ repertoire during β selection is made relevant
369 by findings that the pre-TCR can bind with low affinity to MHC-peptide (Li et al., 2021; Mallis et al.,
370 2015). The pre-TCR also forms an immunological synapse with many similarities to the
371 immunological synapse formed by the αβTCR, oriented towards MHC (Allam et al., 2021). More
372 work is needed to determine any functional connection between CD5 and tuning, or epigenetic
373 modifications during β-selection, but these data point to a role for CD5 during the $DN3b^{Pre}$ stage in
374 reporting pre-TCR activity to determine subsequent passage through the β-selection checkpoint.

375 The molecular basis by which ACY1215 mediates the effects on cell fate we observe here needs
376 more exploration. There are many possible means by which ACY1215 might impact upon
377 transcriptional and epigenetic alterations during β-selection to mediate the phonotypes we observe

378 here. At β-selection, transient activation of β-catenin mediates TCF-1 and Lef1 transcriptional
379 regulation to promote pre-TCR-dependent transition to the DN4 stage (Xu et al., 2009). Ectopic
380 expression of a constitutively active β-catenin allows the cells to bypass pre-TCR signalling, yielding
381 DN4 cells lacking expression of TCRβ (Gounari et al., 2001). The similarities between this phenotype
382 and the apparent bypass of pre-TCR signalling we observe with ACY1215 treatment suggest TCF-
383 1/Lef might mediate the effects of ACY1215. Indeed, HDAC6 can regulate acetylation of β-catenin to
384 coordinate its degradation, providing a possible mechanism for the effects of ACY1215 on TCF-1/Lef
385 activity (Iaconelli et al., 2015). Given the correlation between Lef1 expression and CD5 we observe,
386 CD5 might be downstream of Lef1 during β-selection, perhaps explaining the ACY1215-mediated
387 deregulation of CD5 expression. These findings suggest that the induction of Lef1 at the DN3b^{Pre}
388 stage is coordinated with pre-TCR signalling, in part to promote CD5 expression, and that this activity
389 can be altered by ACY1215 treatment. Whether the effect of ACY1215 relates to HDAC6, an
390 alternative HDAC, or the histone deacetylase activity of Lef1/TCF-1 remains to be determined.

391 Other molecular mediators downstream of ACY1215 effects are also possible. It was recently shown
392 that the transcriptional repressor, Bcl6, is induced by pre-TCR signalling and required for passage
393 through the β-selection checkpoint (Solanki et al., 2020). Differentiation of T follicular helper cells
394 also requires Bcl6, in this case induced by Lef1 and TCF (Choi et al., 2015). Several HDACs have
395 been shown to complex with and modulate Bcl6 activity to impact on B cell development and
396 function (Wang et al., 2020). Together with our findings, these studies suggest the possibility that
397 ACY1215 might mediate at least some of its effects via Bcl6. HDAC6 has also been implicated in the
398 DNA damage response (Zhang et al., 2019), raising the possibility that ACY1215 effects might relate
399 to the genetic recombination integral to the creation of a TCRβ chain (Miyazaki et al., 2008). In any
400 case, the functional outcome of ACY1215 treatment is to disrupt the connections between pre-TCR
401 signalling and expression of CD5 expression and CD5-associated proliferation. Uncoupling CD5 from
402 TCRβ and Lef1 expression provides a possible mechanism by which ACY1215 allows the wrong
403 cells (perhaps cells without suitable TCRβ) to proliferate and differentiate to DN3b^{Post} cells, but these
404 cells subsequently fail to progress, leading to the block in DP differentiation.

405 The known role for HDAC6 in linking tubulin acetylation to the immunological synapse of mature T
406 cells (Serrador et al., 2004), and our finding that acetylation of α-tubulin is increased in DN3 cells,
407 suggested the possibility that the β-selection immunological synapse might mediate the effects of
408 ACY125. Indeed, ACY1215 does alter the organisation of the TCR signalling molecules, LAT,
409 around the MTOC. Similarly, Notch1, which is required to enhance the polarisation of the pre-TCR
410 (Allam et al., 2021; Charnley et al., 2020), is lost from the MTOC following ACY1215 treatment.
411 These findings are particularly interesting in light of a recent report that HDAC6 is required for the
412 formation of aggresomes at the MTOC (Magupalli et al., 2020), and suggest that HDAC6 might play
413 a more general role in coordinating recruitment to the MTOC. An alternative explanation for the
414 effect of ACY1215 on β-selection relates to observations that HDAC inhibitors can induce MHC
415 constituents to promote antigen presentation (Magner et al., 2000). It remains to be determined
416 whether an influence on stromal-presented peptide-MHC plays any role in disrupting β-selection.
417 Interestingly, both CD2 and CD5 can regulate activity of the immunological synapse and connectivity
418 to the MTOC (Brossard et al., 2003; Dustin et al., 1998; Tibaldi et al., 2002) further supporting the
419 possibility that the immunological synapse provides a hub at which deacetylation and pre-TCR
420 signalling converge. Together, these findings suggest that the effect of HDAC6 on β-selection that we
421 see here might occur through disruption of the DN3 immunological synapse.

422 The molecular basis for the effects of ACY1215 on β-selection might therefore by multifaceted, and
423 relate to one or more of direct alteration of the epigenome to influence protein expression, alteration
424 of Lef1 activity, DNA damage response, alteration of pre-TCR signalling via organisation at the
425 MTOC and the immunological synapse. Irrespective of the molecular mechanism, the finding that
426 AY1215 disrupts T cell development has potential implications for the development of clinical
427 applications of small molecule inhibitors of HDAC6, particularly in treatment of young patients,
428 whose T cell repertoire has not yet been established (Cosenza and Pozzi, 2018; Hogg et al., 2020).

429

430 **Materials and Methods**

431 ***Ex vivo* culture of developing T cells and drug treatments**

432 Two sources to derive developing T cells were employed in this study: mouse hematopoietic stem
433 cells (HSCs) and mouse primary thymocytes. HSCs were collected from C57BL/6 mouse E14.5
434 fetal liver. To induce *ex vivo* T cell development, HSCs were co-cultured with OP9-DL1 stromal
435 cells (from Juan Carlos Zúñiga-Pflücker, University of Toronto, Toronto, Canada) at a 1:1 ratio in a
436 6-well plate (2×10^5). The coculture was maintained in αMEM (Sigma-Aldrich, M4526),
437 supplemented with foetal calf serum (10% v/v), glutamine (1 mM), β-mercaptoethanol (50 μM),
438 sodium pyruvate (1nM), HEPES (10 mM), penicillin/streptomycin (100 ng/mL), mouse interleukin 7
439 (1 ng/mL) and mouse FMS-like tyrosine kinase 3 (5 ng/ml). C57BL/6 mice at 4-5 week were
440 euthanised for thymus collection. The primary thymocytes were released from thymus for sorting,
441 analysis or further culturing with OP9-DL1 stromal cells under the same culture conditions as the
442 HSC system described above. For both sources of developing T cells, ACY1215, purchased from
443 MedChemExpress (NJ, USA), was used at 1 μM as described (Laino et al., 2019). ACY1215 was
444 dissolved in DMSO to 5 mM, and diluted to 1 μM with culture media immediately prior to application
445 to cells. The small-molecule inhibitor of Stat5, Pimozide (CAS 2062-78-4 Sigma-Aldrich) was used
446 at a final concentration of 10 μM. The selective inhibitor of p300 and CBP, C646 (Sigma-Aldrich)
447 was used at 2.5 μM. OP9-DL1 stromal cells was maintained in αMEM (Sigma-Aldrich, M4526)
448 supplemented with 20% (v/v) fetal calf serum, glutamine (1 mM) and penicillin/streptomycin (100
449 ng/mL). When OP9-DL1 stromal cells were confluent after 3-4 days of coculture, primary thymocytes
450 were dissociated from the stromal cells through forceful pipetting, and were harvested with the fresh
451 OP9-DL1 stromal cells.

452 **Flow Cytometry and FACS**

453 To purify T cell populations using flow cytometry, primary thymocytes were dissociated from OP9-
454 DL1 stromal cell, and were resuspended in PBS buffer containing 2% FBS and antibody cocktail for
455 surface staining. Antibody cocktails were comprised of lineage markers (NK-1.1, CD11b, CD45R,
456 Ly6G6C, Ter119), and differentiation markers (CD4, CD8, CD25, CD44, CD28 and CD2; details
457 about fluorochrome, manufacturer and dilution are summarised in the supplementary materials).
458 Primary thymocytes were incubated with antibody cocktails for 40 minutes before FACS.

459 Flow cytometry (BD Aria III) was used to analyse and sort the populations of developing T cells.
460 DN3 cells were identified based on surface expression (Lineage^{-}, CD4^{-}, CD8^{-}, CD25^{Hi}, CD44^{Lo}).
461 DN3a cells were DN3 cell with CD28^{L0}, by contrast, DN3b cells were DN3 cell with CD28^{Hi}. DP
462 cells were identified based on surface expression (Lineage^{-}, CD4^{+}, CD8^{+}).

463 **Intracellular staining for flow cytometry**

464 To detect intracellular expression of TCRβ, Ki67, Lef1, c-Myc, Notch1, HDAC6 and H3K18ac, the
465 Foxp3/Transcription Factor Staining Buffer Kit (eBioscience) was used according to the
466 manufacturer's instruction. Briefly, the primary thymocytes after surface staining were incubated with
467 fixative for 15 minutes in dark, room temperature, followed with centrifuge and washing out the
468 fixative. To detect expression of acetyl-tubulin, the cells were fixed with IC Fixation Buffer
469 (eBioscience) for 15 minutes in dark, room temperature, followed with centrifuge and washing out the
470 fixative. The fixed cells were then incubated with antibody for flow cytometry analysis.

471 **Immunofluorescence staining and confocal microscopy**

472 The sorted DN3a or DN3b were grown on glass-bottomed 8-well chambers (ibidi) with OP9-DL1
473 stromal cells, and were fixed with 4% formaldehyde for 8 minutes at room temperature followed by
474 0.1% Triton X-100 permeabilization for 5 minutes. The samples were then incubated with primary
475 antibody overnight at 4°C (details about antibody usage is summarised in Supplementary table 1).
476 After the primary antibody being washed out by PBS, the cells were labelled with fluorochrome-
477 conjugated secondary antibodies (as Table S1), DAPI (Thermo Fisher Scientific), and Phalloidin
478 (Abcam). The samples were examined using a FV3000 confocal microscope (Olympus) and 60X lens
479 (1.30 NA, UPLSAPO, Olympus). The images were processed with maximum intensity projection
480 using Image J. The mean intensity of region of interest was examined in Image J.

481 **Data collection and Statistical analyses**

482 Python (version 3.8.1) was used to visualise the statistics. Data of flow cytometry were analysed by
483 FlowJo software (version X10.0.7r2. Tree Star, Inc.). The bar plot was shown as mean ± SEM. More

484 than three repeats were included in the statistics and were colour-coded for each individual repeat.

485 Microsoft Excel (version 2016) was used for two sided t-test, by which p value was indicated.

486

Acknowledgements

This work was done on Wurundjeri land of the Kulin nation, and we pay our respects to the Elders past and present. We thank Louise Cheng, Callum Dark, Amr Allam and Peter Fraser for technical assistance and helpful discussions, and Ellis Reinherz, Jonathon Duke-Cohan for helpful comments on the manuscript. The work was funded by Australian Research Council (FT0990405 to SMR), National Health and Medical Research Council (APP1099140 to SMR), Swinburne University Postgraduate Research Award to ASC.

Competing Interest Statement

No author declares any competing interests

Author Contribution Statement

Conceptualization: ASC, SMR
Methodology: ASC, MC, SMR
Experimentation: ASC
Visualization: ASC, SMR
Supervision: POH, RWJ, SMR
Writing—original draft: ASC, SMR
Writing—review & editing: ASC, MC, LN, AN, POH, RWJ, SMR

Ethics

C57bl/6 mouse E14.5 fetal livers and 4-5-week mouse thymi were collected according to Peter MacCallum Cancer Centre Ethics Committee approval E627 and La Trobe University Animal Ethics Committee approval AEC-20024.

Figure Legends

Figure 1. ACY1215 inhibits T cell development at the DN3 stage

516 **(A)** FL-derived developing T cells were treated with ACY1215 or DMSO for 2 days as indicated, and
517 the Lin^- cells were assessed for CD4 and CD8 expression to determine the proportions of DN, DP,
518 $CD8^+$ and $CD4^+$ populations. The DN (Lin^-, $CD4^-$, $CD8^-$) cells were assessed for CD44 and CD25
519 expression to determine the proportions of DN3 and DN4 populations. The frequency of each
520 population was summarised in a swarm plot, with individual colours representing each experiment.

521 Sorted, FL-derived DN3a cells **(B)** or thymocytes **(C)** were cultured under ACY1215 or DMSO
522 treatment for 1 or 2 days as indicated, and the $CD44^-$ DN population (representing DN3 and DN4
523 stages) was assessed for CD25 and CD28 expression. The frequency of each population were
524 summarised in swarm plots, with individual colours representing each experiment. Cell numbers were
525 summarised in line plots.

526 **(D)** Sorted, FL-derived DN3b cells were cultured for 4 days under ACY1215 or DMSO treatment as
527 indicated, and cell numbers per population were estimated by multiplying the total cell number by the
528 frequency and were summarised in the line chart.

529

530 **Figure 2. ACY1215 inhibits β-selection.**

531 **(A)** Developing T cells from FL **(i)** or the adult thymus **(ii)** were treated with ACY1215 or DMSO for
532 1 day or 2 days, and the DN3 cells were assessed for CD27 and CD28 expression to discriminate
533 DN3a and DN3b. Cell number or frequency were summarised in the swarm plot, with individual
534 colours representing each experiment.

535 **(B)** Sorted, FL-derived DN3a cells **(i)** were cultured under ACY1215 or DMSO treatment for 4 days
536 as indicated, and DN3 cells were assessed for the expressions of intracellular TCRβ (icTCRβ) versus
537 CD28 or CD27. Thymocytes **(ii)** were cultured under ACY1215 or DMSO treatment for 1 day as
538 indicated, and DN3 cells were assessed for the expressions of icTCRβ versus CD28. The frequency of
539 $icTCR\beta^+$ cells was summarised in a swarm plot, with individual colours representing each experiment.

540

541 **Figure 3. CD2 upregulation discriminates DN3b^{Pre} and DN3b^{Post} populations**

542 **(A)** The strategy for discriminating between three populations (DN3a, DN3b^{Pre}, and DN3b^{Post}) is
543 indicated in the schematic.

544 **(B)** FL-derived developing T cells **(i)** or the sorted thymocyte DN3 **(ii)** were treated with ACY1215
545 or DMSO for 1 or 2 days, and the DN3 cells were assessed for CD2 and CD28 expression.

546 **(C)** FL-derived developing T cells **(i)** or the sorted thymus-derived DN3 **(ii)** were treated with
547 ACY1215 or DMSO for 1 day, and DN3a, DN3b^{Pre}, and DN3b^{Post} cells were assessed for icTCRβ and
548 Ki-67 expression. MFI of icTCRβ and Ki-67 were summarised in histogram and swarm plot, with
549 individual colours representing each experiment. (p value < 0.001 = '***', < 0.01 = '**', <0.05 ='*')

550

551 **Figure 4. DN3a, DN3b^{Pre} and DN3b^{Post} stages follow a sequential progression.**

552 The DN3a, DN3b^{Pre}, and DN3b^{Post} cells from the adult thymus were sorted as indicated, and were
553 cultured on OP9-DL1. At two day, the cells were analysed by CD4 versus CD8, the DN cells were
554 analysed by CD44 versus CD25, and the DN3 cells were analysed by CD2 versus CD28. The
555 frequencies of each population were summarised in the line plots. (p value < 0.001 = '***', < 0.01 =
556 '**', <0.05 ='*')

557

558 **Figure 5. ACY1215 alters pre-TCR signalling clustered at the MTOC.**

559 **(A)** Sorted FL-derived DN, DP, CD4-SP, CD8-SP, DN1, DN2, DN3a, DN3b were treated with
560 ACY1215 or DMSO for 2 hours as indicated, and were assessed for acetyl-α-tubulin (K40) as shown
561 in histograms.

562 **(B, C)** Sorted FL-derived DN3a cells were treated with ACY1215 or DMSO for 1 day as indicated,
563 followed by immunostaining for LAT, acetyl-α-tubulin (K40), Notch1 and α-tubulin. The mean
564 intensity of acetyl-α-tubulin, LAT and the ratio of Notch1 expressed at MTOC versus at nucleus were

565 summarized in violin plot overlaid with box plot. Cell number for LAT staining: ACY1215 (n=55)
566 and DMSO (n=54); Cell number for acetyl-α-tubulin (K40) staining: ACY1215 (n=30) and DMSO
567 (n=31); Cell number for Notch1 staining: ACY1215 (n=56) and DMSO (n=55).

568 **(D)** FL-derived developing T cells were treated with ACY1215 or DMSO for 2 day, and the DN3a,
569 DN3b and DN4 cells were assessed for Notch1 expression, as summarised in swarm plot, with
570 individual colours representing each experiment.

571

572 **Figure 6. Coordinated upregulation of Lef1 and TCRβ in DN3b^{Pre} cells.**

573 **(A)** FL-derived developing T cells **(i)** or the sorted thymocyte DN3 **(ii)** were treated with ACY1215 or
574 DMSO for 1 day as indicated, and DN3 cells were assessed for CD2 and CD28 expression. The
575 DN3a, DN3b^{Pre}, and DN3b^{Post} cells were assessed for Lef1 expression.

576 **(B)** DN3a, DN3b^{Pre}, and DN3b^{Post} cells from (A, i) were assessed for Lef1 and icTCRβ expression.

577

578 **Figure 7. CD5 is upregulated with Lef1 and TCRβ in DN3b^{Post} cells.**

579 **(A)** Sorted DN3 cells from the adult thymus were treated with ACY1215 or DMSO for 1 day as
580 indicated, and DN3 cells were assessed for CD5, CD2 and Lef1 expression.

581 **(B)** Sorted DN3a and DN3b^{Pre} cells from the adult thymus were treated with ACY1215 or DMSO for
582 2 day as indicated, and DN3 populations were assessed for CD5 and surface TCRβ expression.

583 (C) Schematic describes the stepwise expression of TCR co-receptors (CD28, CD5, and CD2) and
584 Lef1 from DN3a, DN3b^{Pre} to DN3b^{Post} stage.

585

586 **Figure 8. CD5 upregulation correlates with the passing of β-selection checkpoint**

587 **(A)** Sorted FL-derived DN3a and DN3b were stained with CFSE after sorting and were cultured with
588 ACY1215 or DMSO for two days as indicated. At two days, the DN3a, DN3b^{Pre}, and DN3b^{Post} cells
589 from the sorted DN3a and DN3b were assessed for CD5 expression versus CFSE intensity.

590 **(B)** Schematic summarises the working model of molecular interactions at the DN3b^{Pre} stage. Firstly,
591 CD28 (the defining step in transition from DN3a to DN3b^{Pre}) acts to promote signalling through the
592 nascent pre-TCR. Second, pre-TCR signals induce expression of CD5 (or *vice versa*) and lead to the
593 passing of the β-selection checkpoint. By coordinating transcriptional control, functional MTOC and
594 immunological synapse formation for survival, proliferation and differentiation. Possible molecular
595 events disrupted by ACY1215 treatment to cause these cellular responses are indicated by the red
596 double lines.

597

598 **Figure S1.**

599 **(A)** A schematic of the stages of T cell development and the cell surface markers used to differentiate
600 them. Cells were classed as DN (Double Negative, lacking expression of CD4 and CD8), and
601 progressed from DN1 to DN4 according to their expression of CD44 and CD25 as indicated. β-
602 selection occurs at the DN3 stage, as cells progress from DN3a to DN3b, indicated by upregulation of
603 CD28. Cells post β-selection progressed from DN4 to the DP stage (Double Positive, expressing both
604 CD4 and CD8) before committing to SP (Single Positive for either CD4 or CD8).

605 **(B)** Fetal liver cells were collected from E14.5 mice embryos, and cells cultured on OP9-D1L stromal
606 cells for 8-10 days. The developing T cells were demarcated as the flow indicated.

607 **(C)** Thymocytes were collected from 4-to-5-week mice thymus **(i)** and/or were cultured *ex vivo* on
608 OP9-DL1 stromal cells **(ii)**. The developing T cells were demarcated as the flow indicated.

609

610 **Figure S2.**

611 Sorted, FL-derived DN2, DN3a, DN3b and DP were cultured for 2 days ACY1215 or DMSO
612 treatment as indicated. Cell numbers were counted at 3 hours and 2 days, and the proliferation rate (2
613 days / 3 hours) was summarised in swarm plot, with individual colours representing independent
614 experiments.

615

616 **Figure S3.**

617 **(A)** Sorted, FL-derived DN3a and DN3b were stained with CFSE after sorting and were cultured with
618 ACY1215 or DMSO for two days as indicated. At one hour post sorting, the intensity of CFSE were
619 recorded, as indicated by the white histogram. At two days, the DN3 cells from the sorted DN3a and
620 DN3b were assessed for CD28 expression and CFSE intensity, as shown in the contour plots and the
621 histograms.

622 **(B)** FL-derived developing T cells were treated with ACY1215 or DMSO for 1 day as indicated, and
623 DN3a and DN3b cells were assessed for FSC and Ki-67 expression.

624

625 **Figure S4.**

626 **(A)** Sorted, FL-derived DN3a, DN3b and DP cells were treated with ACY1215 or DMSO for 3 hours
627 or 6 hours as indicated, followed with propidium iodide (PI) staining to label dead cells. The
628 frequency of PI^+ population were summarised in swarm plot, with individual colours representing
629 each experiment.

630 **(B)** Sorted, FL-derived DN3a and DN3b cells were treated with ACY1215 or DMSO for 6 hours or 1
631 day with or without OP9-DL1 coculture as indicated. The cells were assessed for Annexin V
632 expression and DAPI intensity as shown in the density plot.

633

634 **Figure S5.**

635 Sorted, FL-derived DN3a **(A)** and sorted, FL-derived DN3b **(B)** were cultured for 4 days under
636 ACY1215 or DMSO treatment as indicated, and were analysed by CD4 and CD8 **(i)** and CD44 and
637 CD25 **(ii)**. The frequency of each population was summarised in swarm plot, with individual colours
638 representing independent experiments.

639

640 **Figure S6.**

641 **(A)** FL-derived developing T cells were treated with ACY1215 or DMSO for 2 days as indicated, and
642 DN3a, DN3b, DN4 and DP cells were assessed for surface TCRβ and surface TCRγδ expression. **(B)**
643 Sorted, FL-derived DN3b cells were cultured for 2 days under ACY1215 or DMSO treatment as
644 indicated, and DN3, DN4 and DP cells were assessed for surface TCRβ and surface TCRγδ
645 expression. **(C)** Sorted FL-derived DN3b cells were cultured for 4 days under ACY1215 or DMSO
646 treatment as indicated, and DN3, DN4 and DP cells were assessed for intracellular TCRβ (icTCRβ)
647 and CD28 expression. The frequency and cell number were summarised in swarm plot, with
648 individual colours representing each experiment.

649

650 **Figure S7.**

651 **(A)** CD28 upregulation marks both DN3 cells differentiation and passing β-selection. FL-derived
652 developing T cells at around day 8-10 of coculture with OP9-DL1 stromal cells were assessed for
653 CD28, CD71, CD98, CD27 and surface TCRβ expression.

654 **(B)** Sorted, FL-derived DN3b **(i)** or thymocytes **(ii)** were treated with ACY1215 or DMSO for 1 day
655 or 2 days as indicated, and the DN3 cells were assessed for surface TCRβ and icTCRβ expression.
656 MFI of surface TCRβ from icTCRβ^{+} cells was summarised in a swarm plot, with individual colours
657 representing each experiment.

658

659 **Figure S8**

660 **(A)** Quantification for Figure 3A. Frequency and cell number of the three populations (DN3a,
661 DN3b^{Pre}, and DN3b^{Post}) was summarised in swarm plots, with individual colours representing each
662 experiment.

663 **(B)** Sorted, FL-derived DN3a and DN3b were stained with CFSE after sorting and were cultured with
664 ACY1215 or DMSO for two days as indicated. At two days, the DN3 cells from the sorted DN3a and
665 DN3b were assessed for CD2 expression versus CFSE intensity.

666 **(C)** DN3a, DN3b^{Pre}, and DN3b^{Post} thymocytes that treated with ACY1215 for 1 day were assessed for
667 CD27 and surface TCRβ expression.

668 **(D)** FL-derived developing T cells were treated with ACY1215 or DMSO for 2 days, and DN3a,
669 DN3b^{Pre}, and DN3b^{Post} cells were assessed for c-Myc expression.

670

671 **Figure S9**

672 FL-derived developing T cells were treated with DMSO or ACY1215 for 1.5 day, and DN3a,
673 DN3b^{Pre}, and DN3b^{Post} cells were sorted as indicated **(i)**. At one day, the cells were analysed by CD4
674 versus CD8 **(ii)** and CD2 versus CD28 **(iii)**. The frequencies of each population were summarised in
675 the line plots. (p value < 0.001 = '***', < 0.01 = '**', <0.05 ='*')

676

677

678 **Figure S10.**

679 HDAC6 is expressed in developing T cells. **(A)** To examine HDAC6 protein expression, FL-derived
680 developing T cells treated with DMSO or ACY1215 for two days were fixed by cytoplasmic fixative
681 or nuclear fixative, followed by examination of HDAC6 expression. **(B)** FL-derived developing T
682 cells were treated with ACY1215, the selective inhibitor of p300 and CBP, C646, or DMSO for 1 day
683 as indicated, and the expression of H3K18ac were assessed and shown in the histogram. **(C)** Sorted,

684 FL-derived DN3a or DN3b cells were assessed for HDAC6 (in white colour) expression by
685 immunostaining. **(D, E)** Sorted, FL-derived DN3b cells were treated with ACY1215 or DMSO for 1
686 day, followed by immunostaining for α-tubulin, Arp2 (in white colour), acetyl-α-tubulin (K40) (in
687 white colour).

688

689

690 **Figure S11.**

691 FL-derived developing T cells were treated with ACY1215 or DMSO for 1 day as indicated, and
692 DN3a, DN3b^{Pre}, and DN3b^{Post} cells were assessed for Lef1 and CD2 expression. DN3b^{Pre} cells were
693 further characterised by Lef1^{Hi} or Lef1^{Lo}, and were assessed for Lef1 and CD5 expression with DN3a
694 and DN3b^{Post}.

695

696 **Figure S12.**

697 **(A)** Sorted FL-derived DN3b^{Pre} cells were accessed for CD25 expression as schematic indicated.

698 **(B)** FL-derived developing T cells were treated with ACY1215 or DMSO for 2 days as indicated, and
699 DN3a and DN3b were assessed for Lef1 and CD5 expression. The expression of CD25 in the DN3b
700 subsets were shown in histogram.

701 **Figure S13.**

702 Sorted FL-derived DN3a and DN3b cells were treated with DMSO or ACY1215 for 2 days, and were
703 assessed for CD5, TCRβ and CD25 expression.

704

705 **Figure S14.**

706 Schematic shows the sequence of protein expression changes during development from DN3a,

707 $DN3b^{Pre}$ to $DN3b^{Post}$.

708

709

710 Adeegbe, D.O., Y. Liu, P.H. Lizotte, Y. Kamihara, A.R. Aref, C. Almonte, R. Dries, Y. Li, S. Liu, X. Wang,
711 T. Warner-Hatten, J. Castrillon, G.C. Yuan, N. Poudel-Neupane, H. Zhang, J.L. Guerriero, S.
712 Han, M.M. Awad, D.A. Barbie, J. Ritz, S.S. Jones, P.S. Hammerman, J. Bradner, S.N. Quayle,
713 and K.K. Wong. 2017. Synergistic Immunostimulatory Effects and Therapeutic Benefit of
714 Combined Histone Deacetylase and Bromodomain Inhibition in Non-Small Cell Lung Cancer.
715 *Cancer discovery* 7:852-867.
716 Allam, A.H., M. Charnley, K. Pham, and S.M. Russell. 2021. Developing T cells form an immunological
717 synapse for passage through the beta-selection checkpoint. *J Cell Biol* 220:
718 Ananias, H.J., I.J. de Jong, R.A. Dierckx, C. van de Wiele, W. Helfrich, and P.H. Elsinga. 2008. Nuclear
719 imaging of prostate cancer with gastrin-releasing-peptide-receptor targeted
720 radiopharmaceuticals. *Current pharmaceutical design* 14:3033-3047.
721 Azzam, H.S., J.B. DeJarnette, K. Huang, R. Emmons, C.-S. Park, C.L. Sommers, D. El-Khoury, E.W.
722 Shores, and P.E. Love. 2001. Fine Tuning of TCR Signaling by CD5. *The Journal of Immunology*
723 166:5464-5472.
724 Azzam, H.S., A. Grinberg, K. Lui, H. Shen, E.W. Shores, and P.E. Love. 1998. CD5 expression is
725 developmentally regulated by T cell receptor (TCR) signals and TCR avidity. *J Exp Med*
726 188:2301-2311.
727 Bachmann, M.F., M. Barner, and M. Kopf. 1999. CD2 sets quantitative thresholds in T cell activation.
728 *J Exp Med* 190:1383-1392.
729 Ballesteros-Arias, L., J.G. Silva, R.A. Paiva, B. Carbonetto, P. Faisca, and V.C. Martins. 2019. T Cell
730 Acute Lymphoblastic Leukemia as a Consequence of Thymus Autonomy. *J Immunol*
731 Brossard, C., M. Semichon, A. Trautmann, and G. Bismuth. 2003. CD5 inhibits signaling at the
732 immunological synapse without impairing its formation. *J Immunol* 170:4623-4629.
733 Chann, A.S., and S.M. Russell. 2019. An integrated transcriptional switch at the beta-selection
734 checkpoint determines T cell survival, development and leukaemogenesis. *Biochemical*
735 *Society transactions* 47:1077-1089.
736 Charnley, M., M. Ludford-Menting, K. Pham, and S.M. Russell. 2020. A new role for Notch in the
737 control of polarity and asymmetric cell division of developing T cells. *J Cell Sci* 133:jcs235358.
738 Choi, Y.S., J.A. Gullicksrud, S. Xing, Z. Zeng, Q. Shan, F. Li, P.E. Love, W. Peng, H.H. Xue, and S. Crotty.
739 2015. LEF-1 and TCF-1 orchestrate T differentiation by regulating differentiation circuits
740 upstream of the transcriptional repressor Bcl6. *Nat Immunol*
741 Cosenza, M., and S. Pozzi. 2018. The Therapeutic Strategy of HDAC6 Inhibitors in
742 Lymphoproliferative Disease. *International journal of molecular sciences* 19:
743 Dose, M., I. Khan, Z. Guo, D. Kovalovsky, A. Krueger, H. von Boehmer, K. Khazaie, and F. Gounari.
744 2006. c-Myc mediates pre-TCR-induced proliferation but not developmental progression.
745 *Blood* 108:2669-2677.
746 Douek, D.C., R.A. Vescio, M.R. Betts, J.M. Brenchley, B.J. Hill, L. Zhang, J.R. Berenson, R.H. Collins,
747 and R.A. Koup. 2000. Assessment of thymic output in adults after haematopoietic stem-cell
748 transplantation and prediction of T-cell reconstitution. *Lancet* 355:1875-1881.
749 Dustin, M.L., M.W. Olszowy, A.D. Holdorf, J. Li, S. Bromley, N. Desai, P. Widder, F. Rosenberger, P.A.
750 van der Merwe, P.M. Allen, and A.S. Shaw. 1998. A novel adaptor protein orchestrates
751 receptor patterning and cytoskeletal polarity in T-cell contacts. *Cell* 94:667-677.

752 Dutta, A., B. Zhao, and P.E. Love. 2021. New insights into TCR β-selection. *Trends in Immunology*
753 Eich, C., J. Arlt, C.S. Vink, P. Solaimani Kartalaei, P. Kaimakis, S.A. Mariani, R. van der Linden, W.A. van
754 Cappellen, and E. Dzierzak. 2018. In vivo single cell analysis reveals Gata2 dynamics in cells
755 transitioning to hematopoietic fate. *The Journal of Experimental Medicine* 215:233-248.
756 Gounari, F., I. Aifantis, K. Khazaie, S. Hoeflinger, N. Harada, M.M. Taketo, and H. von Boehmer. 2001.
757 Somatic activation of beta-catenin bypasses pre-TCR signaling and TCR selection in
758 thymocyte development. *Nat Immunol* 2:863-869.
759 Goux, D., J.D. Coudert, D. Maurice, L. Scarpellino, G. Jeannet, S. Piccolo, K. Weston, J. Huelsken, and
760 W. Held. 2005. Cooperating pre-T-cell receptor and TCF-1-dependent signals ensure
761 thymocyte survival. *Blood* 106:1726-1733.
762 Groettrup, M., A. Baron, G. Griffiths, R. Palacios, and H. von Boehmer. 1992. T cell receptor (TCR)
763 beta chain homodimers on the surface of immature but not mature alpha, gamma, delta
764 chain deficient T cell lines. *EMBO J* 11:2735-2745.
765 Hayday, A.C., and D.J. Pennington. 2007. Key factors in the organized chaos of early T cell
766 development. *Nat Immunol* 8:137-144.
767 Hogg, S.J., P.A. Beavis, M.A. Dawson, and R.W. Johnstone. 2020. Targeting the epigenetic regulation
768 of antitumour immunity. *Nature reviews. Drug discovery*
769 Holmes, R., and J.C. Zúñiga-Pflücker. 2009. The OP9-DL1 system: generation of T-lymphocytes from
770 embryonic or hematopoietic stem cells in vitro. *Cold Spring Harb Protoc* 2009:pdb.prot5156.
771 Iaconelli, J., J.H. Huang, S.S. Berkovitch, S. Chattopadhyay, R. Mazitschek, S.L. Schreiber, S.J.
772 Haggarty, and R. Karmacharya. 2015. HDAC6 inhibitors modulate Lys49 acetylation and
773 membrane localization of beta-catenin in human iPSC-derived neuronal cells. *ACS Chem Biol*
774 10:883-890.
775 Kamoun, M., J.S. Woods, N. Sano, H. Makni, R. Smith, W.B. de Lau, A. van Oers, D. Wotton, M.J.
776 Owen, Y. Hashimoto, and H.C. Clevers. 1995. Analysis of CD2 and TCR-beta gene expression
777 in Jurkat cell mutants suggests a cis regulation of gene transcription. *J Immunol* 155:3929-
778 3937.
779 Laino, A.S., B.C. Betts, A. Veerapathran, I. Dolgalev, A. Sarnaik, S.N. Quayle, S.S. Jones, J.S. Weber,
780 and D.M. Woods. 2019. HDAC6 selective inhibition of melanoma patient T-cells augments
781 anti-tumor characteristics. *Journal for immunotherapy of cancer* 7:33.
782 Li, X., R. Mizsei, K. Tan, R.J. Mallis, J.S. Duke-Cohan, A. Akitsu, P.W. Tetteh, A. Dubey, W. Hwang, G.
783 Wagner, M.J. Lang, H. Arthanari, J.H. Wang, and E.L. Reinherz. 2021. Pre-T cell receptors
784 topologically sample self-ligands during thymocyte beta-selection. *Science* 371:181-185.
785 López-Rodríguez, C., J. Aramburu, and R. Berga-Bolaños. 2015. Transcription factors and target genes
786 of pre-TCR signaling. *Cellular and Molecular Life Sciences* 72:2305-2321.
787 Lutes, L.K., Z. Steier, L.L. McIntyre, S. Pandey, J. Kaminski, A.R. Hoover, S. Ariotti, A. Streets, N. Yosef,
788 and E.A. Robey. 2021. T cell self-reactivity during thymic development dictates the timing of
789 positive selection. *eLife* 10:e65435.
790 Magner, W.J., A.L. Kazim, C. Stewart, M.A. Romano, G. Catalano, C. Grande, N. Keiser, F. Santaniello,
791 and T.B. Tomasi. 2000. Activation of MHC class I, II, and CD40 gene expression by histone
792 deacetylase inhibitors. *J Immunol* 165:7017-7024.
793 Magupalli, V.G., R. Negro, Y. Tian, A.V. Hauenstein, G. Di Caprio, W. Skillern, Q. Deng, P. Orning, H.B.
794 Alam, Z. Maliga, H. Sharif, J.J. Hu, C.L. Evavold, J.C. Kagan, F.I. Schmidt, K.A. Fitzgerald, T.
795 Kirchhausen, Y. Li, and H. Wu. 2020. HDAC6 mediates an aggresome-like mechanism for
796 NLRP3 and pyrin inflammasome activation. *Science* 369:eaas8995.
797 Mallis, R.J., K. Bai, H. Arthanari, R.E. Hussey, M. Handley, Z. Li, L. Chingozha, J.S. Duke-Cohan, H. Lu,
798 J.H. Wang, C. Zhu, G. Wagner, and E.L. Reinherz. 2015. Pre-TCR ligand binding impacts
799 thymocyte development before alphabetaTCR expression. *Proc Natl Acad Sci U S A*
800 112:8373-8378.

801 Matson, C.A., S. Choi, F. Livak, B. Zhao, A. Mitra, P.E. Love, and N.J. Singh. 2020. CD5 dynamically
802 calibrates basal NF-kappaB signaling in T cells during thymic development and peripheral
803 activation. *Proc Natl Acad Sci U S A* 117:14342-14353.
804 Mingueneau, M., T. Kreslavsky, D. Gray, T. Heng, R. Cruse, J. Ericson, S. Bendall, M.H. Spitzer, G.P.
805 Nolan, K. Kobayashi, H. von Boehmer, D. Mathis, C. Benoist, C. Immunological Genome, A.J.
806 Best, J. Knell, A. Goldrath, V. Jojic, D. Koller, T. Shay, A. Regev, N. Cohen, P. Brennan, M.
807 Brenner, F. Kim, T.N. Rao, A. Wagers, T. Heng, J. Ericson, K. Rothamel, A. Ortiz-Lopez, D.
808 Mathis, C. Benoist, N.A. Bezman, J.C. Sun, G. Min-Oo, C.C. Kim, L.L. Lanier, J. Miller, B. Brown,
809 M. Merad, E.L. Gautier, C. Jakubzick, G.J. Randolph, P. Monach, D.A. Blair, M.L. Dustin, S.A.
810 Shinton, R.R. Hardy, D. Laidlaw, J. Collins, R. Gazit, D.J. Rossi, N. Malhotra, K. Sylvia, J. Kang,
811 T. Kreslavsky, A. Fletcher, K. Elpek, A. Bellemare-Pelletier, D. Malhotra, and S. Turley. 2013.
812 The transcriptional landscape of alphabeta T cell differentiation. *Nat Immunol* 14:619-632.
813 Miyazaki, M., K. Miyazaki, M. Itoi, Y. Katoh, Y. Guo, R. Kanno, Y. Katoh-Fukui, H. Honda, T. Amagai,
814 M. van Lohuizen, H. Kawamoto, and M. Kanno. 2008. Thymocyte proliferation induced by
815 pre-T cell receptor signaling is maintained through polycomb gene product Bmi-1-mediated
816 Cdkn2a repression. *Immunity* 28:231-245.
817 Narita, T., B.T. Weinert, and C. Choudhary. 2019. Functions and mechanisms of non-histone protein
818 acetylation. *Nature Reviews Molecular Cell Biology* 20:156-174.
819 Notarangelo, L.D., R. Bacchetta, J.L. Casanova, and H.C. Su. 2020. Human inborn errors of immunity:
820 An expanding universe. *Science Immunology* 5:eabb1662.
821 Osseni, A., A. Ravel-Chapuis, J.-L. Thomas, V. Gache, L. Schaeffer, and B.J. Jasmin. 2020. HDAC6
822 regulates microtubule stability and clustering of AChRs at neuromuscular junctions. *Journal
823 of Cell Biology* 219:
824 Rodewald, H.R., K. Awad, P. Moingeon, L. D'Adamio, D. Rabinowitz, Y. Shinkai, F.W. Alt, and E.L.
825 Reinherz. 1993. Fc gamma RII/III and CD2 expression mark distinct subpopulations of
826 immature CD4-CD8- murine thymocytes: in vivo developmental kinetics and T cell receptor
827 beta chain rearrangement status. *J Exp Med* 177:1079-1092.
828 Rogers, D., A. Sood, H. Wang, J.J.P. van Beek, T.J. Rademaker, P. Artusa, C. Schneider, C. Shen, D.C.
829 Wong, M.-È. Lebel, S.A. Condotta, M.J. Richer, A.J. Martins, J.S. Tsang, L. Barreiro, P.
830 Francois, D. Langlais, H.J. Melichar, J. Textor, and J.N. Mandl. 2021. Pre-existing chromatin
831 accessibility and gene expression differences among naïve CD4⁺ T cells
832 influence effector potential. *bioRxiv* 2021.2004.2021.440846.
833 Sasada, T., and E.L. Reinherz. 2001. A critical role for CD2 in both thymic selection events and mature
834 T cell function. *J Immunol* 166:2394-2403.
835 Serrador, J.M., J.R. Cabrero, D. Sancho, M. Mittelbrunn, A. Urzainqui, and F. Sanchez-Madrid. 2004.
836 HDAC6 deacetylase activity links the tubulin cytoskeleton with immune synapse
837 organization. *Immunity* 20:417-428.
838 Shapiro, M.J., and V.S. Shapiro. 2020. Chromatin-Modifying Enzymes in T Cell Development. *Annu
839 Rev Immunol* 38:397-419.
840 Skånland, Sigrid S., K. Moltu, T. Berge, Einar M. Aandahl, and K. Taskén. 2014. T-cell co-stimulation
841 through the CD2 and CD28 co-receptors induces distinct signalling responses. *Biochemical
842 Journal* 460:399-410.
843 Solanki, A., D.C. Yánez, C.-I. Lau, J. Rowell, A. Barbarulo, S. Ross, H. Sahni, and T. Crompton. 2020.
844 The transcriptional repressor Bcl6 promotes pre-TCR-induced thymocyte differentiation and
845 attenuates Notch1 activation. *Development* 147:dev192203.
846 Sood, A., M.E. Lebel, M. Dong, M. Fournier, S.J. Vobecky, E. Haddad, J.S. Delisle, J.N. Mandl, N.
847 Vrisekoop, and H.J. Melichar. 2021. CD5 levels define functionally heterogeneous
848 populations of naive human CD4(+) T cells. *Eur J Immunol* 51:1365-1376.
849 Staal, F.J., and H.C. Clevers. 2005. WNT signalling and haematopoiesis: a WNT-WNT situation. *Nat
850 Rev Immunol* 5:21-30.

851 Taghon, T., M.A. Yui, R. Pant, R.A. Diamond, and E.V. Rothenberg. 2006. Developmental and
852 molecular characterization of emerging beta- and gammadelta-selected pre-T cells in the
853 adult mouse thymus. *Immunity* 24:53-64.
854 Tarakhovsky, A., S.B. Kanner, J. Hombach, J.A. Ledbetter, W. Muller, N. Killeen, and K. Rajewsky.
855 1995. A role for CD5 in TCR-mediated signal transduction and thymocyte selection. *Science*
856 269:535-537.
857 Teague, T.K., C. Tan, J.H. Marino, B.K. Davis, A.A. Taylor, R.W. Huey, and C.J. Van De Wiele. 2010.
858 CD28 expression redefines thymocyte development during the pre-T to DP transition. *Int*
859 *Immunol* 22:387-397.
860 Tibaldi, E.V., R. Salgia, and E.L. Reinherz. 2002. CD2 molecules redistribute to the uropod during T
861 cell scanning: implications for cellular activation and immune surveillance. *Proc Natl Acad Sci*
862 *U S A* 99:7582-7587.
863 Travis, A., A. Amsterdam, C. Belanger, and R. Grosschedl. 1991. LEF-1, a gene encoding a lymphoid-
864 specific protein with an HMG domain, regulates T-cell receptor alpha enhancer function
865 [corrected]. *Genes Dev* 5:880-894.
866 Tsuji, G., N. Okiyama, V.A. Villarroel, and S.I. Katz. 2015. Histone deacetylase 6 inhibition impairs
867 effector CD8 T-cell functions during skin inflammation. *J Allergy Clin Immunol* 135:1228-
868 1239.
869 Voisinne, G., A. Gonzalez de Peredo, and R. Roncagalli. 2018. CD5, an Undercover Regulator of TCR
870 Signaling. *Frontiers in Immunology* 9:
871 Wang, P., Z. Wang, and J. Liu. 2020. Role of HDACs in normal and malignant hematopoiesis.
872 *Molecular cancer* 19:5.
873 Williams, J.A., K.S. Hathcock, D. Klug, Y. Harada, B. Choudhury, J.P. Allison, R. Abe, and R.J. Hodes.
874 2005. Regulated costimulation in the thymus is critical for T cell development: dysregulated
875 CD28 costimulation can bypass the pre-TCR checkpoint. *J Immunol* 175:4199-4207.
876 Xing, S., F. Li, Z. Zeng, Y. Zhao, S. Yu, Q. Shan, Y. Li, F.C. Phillips, P.K. Maina, H.H. Qi, C. Liu, J. Zhu,
877 R.M. Pope, C.A. Musselman, C. Zeng, W. Peng, and H.H. Xue. 2016. Tcf1 and Lef1
878 transcription factors establish CD8 T cell identity through intrinsic HDAC activity. *Nat*
879 *Immunol*
880 Xu, K., W.Y. Yang, G.K. Nanayakkara, Y. Shao, F. Yang, W. Hu, E.T. Choi, H. Wang, and X. Yang. 2018.
881 GATA3, HDAC6, and BCL6 Regulate FOXP3+ Treg Plasticity and Determine Treg Conversion
882 into Either Novel Antigen-Presenting Cell-Like Treg or Th1-Treg. *Frontiers in immunology*
883 9:45.
884 Xu, M., A. Sharma, D.L. Wiest, and J.M. Sen. 2009. Pre-TCR-induced beta-catenin facilitates traversal
885 through beta-selection. *J Immunol* 182:751-758.
886 Yashiro-Ohtani, Y., Y. He, T. Ohtani, M.E. Jones, O. Shestova, L. Xu, T.C. Fang, M.Y. Chiang, A.M.
887 Intlekofer, S.C. Blacklow, Y. Zhuang, and W.S. Pear. 2009. Pre-TCR signaling inactivates
888 Notch1 transcription by antagonizing E2A. *Genes Dev* 23:1665-1676.
889 Yu, S., X. Zhou, F.C. Steinke, C. Liu, S.C. Chen, O. Zagorodna, X. Jing, Y. Yokota, D.K. Meyerholz, C.G.
890 Mullighan, C.M. Knudson, D.M. Zhao, and H.H. Xue. 2012. The TCF-1 and LEF-1 transcription
891 factors have cooperative and opposing roles in T cell development and malignancy.
892 *Immunity* 37:813-826.
893 Zhang, M., C. Hu, N. Moses, J. Haakenson, S. Xiang, D. Quan, B. Fang, Z. Yang, W. Bai, G. Bepler, G.M.
894 Li, and X.M. Zhang. 2019. HDAC6 regulates DNA damage response via deacetylating MLH1. *J*
895 *Biol Chem* 294:5813-5826.
896 Zhang, X.-H., M. Qin, H.-P. Wu, M.Y. Khamis, Y.-H. Li, L.-Y. Ma, and H.-M. Liu. 2021. A Review of
897 Progress in Histone Deacetylase 6 Inhibitors Research: Structural Specificity and Functional
898 Diversity. *Journal of medicinal chemistry* 64:1362-1391.
899 Zhang, Y., S. Kwon, T. Yamaguchi, F. Cubizolles, S. Rousseaux, M. Kneissel, C. Cao, N. Li, H.L. Cheng, K.
900 Chua, D. Lombard, A. Mizeracki, G. Matthias, F.W. Alt, S. Khochbin, and P. Matthias. 2008.

901 Mice lacking histone deacetylase 6 have hyperacetylated tubulin but are viable and develop
902 normally. *Mol Cell Biol* 28:1688-1701.
903 Zhao, X., Q. Shan, and H.-H. Xue. 2021. TCF1 in T cell immunity: a broadened frontier. *Nature*
904 *Reviews Immunology*

905

Figure 1.

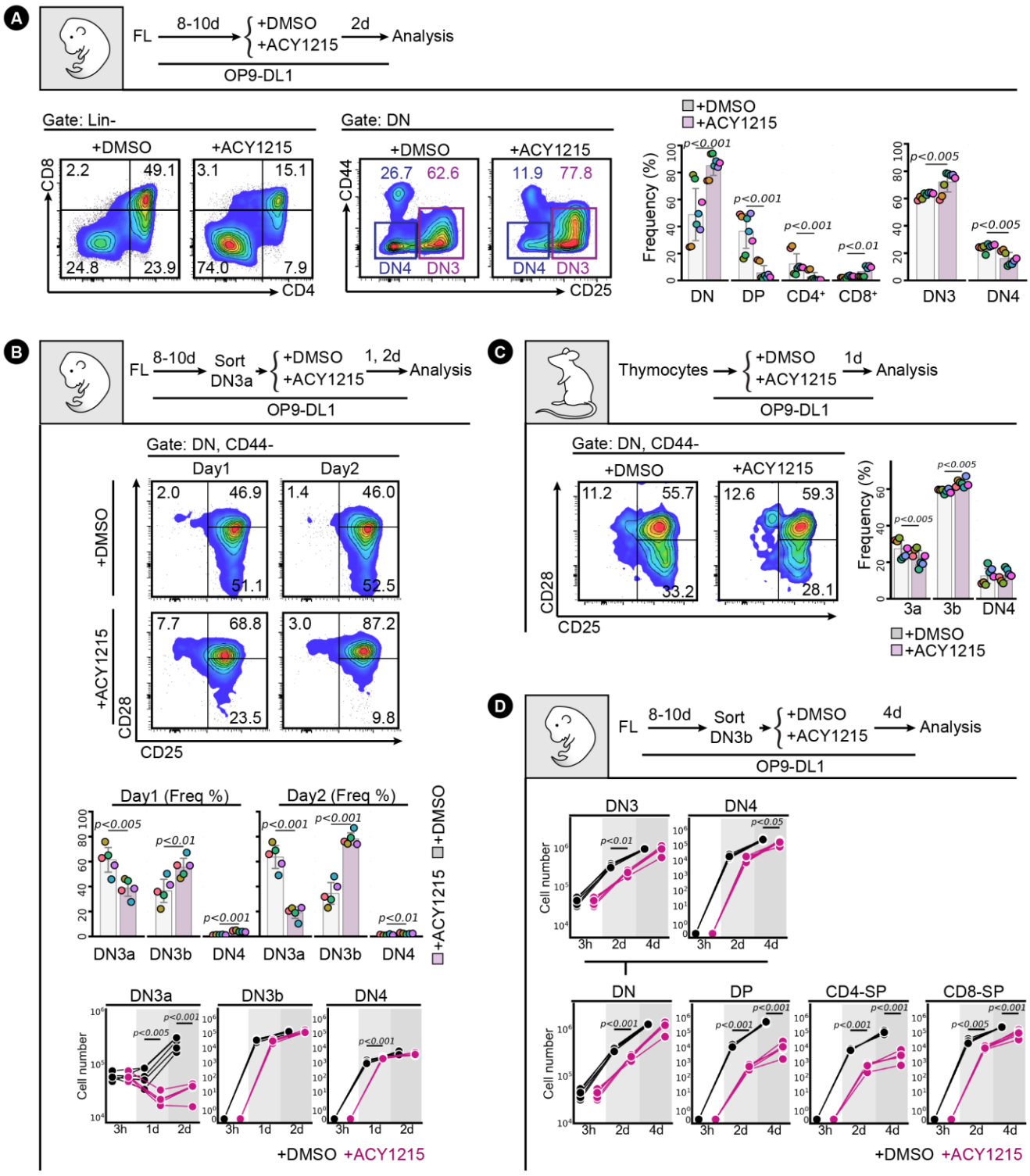
A
FL
8-10d
+DMSO
+ACY1215
2d
Analysis
OP9-DL1
Gate: Lin-
+DMSO
+ACY1215
CD8
CD4
2.2
49.1
24.8
23.9
3.1
15.1
74.0
7.9
Gate: DN
CD44
CD25
26.7
62.6
DN4
DN3
11.9
77.8
Frequency (%)
p<0.001
p<0.01
p<0.005
DN
DP
CD4+
CD8+
DN3
DN4
B
8-10d
Sort
DN3a
1, 2d
Gate: DN, CD44-
Day1
Day2
CD28
CD25
2.0
46.9
51.1
1.4
46.0
52.5
7.7
68.8
23.5
3.0
87.2
9.8
Day1 (Freq %)
Day2 (Freq %)
DN3a
DN3b
DN4
Cell number
3h
1d
2d
C
Thymocytes
1d
Gate: DN, CD44-
11.2
55.7
33.2
12.6
59.3
28.1
3a
3b
D
8-10d
Sort
DN3b
4d
p<0.05
CD4-SP
CD8-SP
4d

Figure 2.

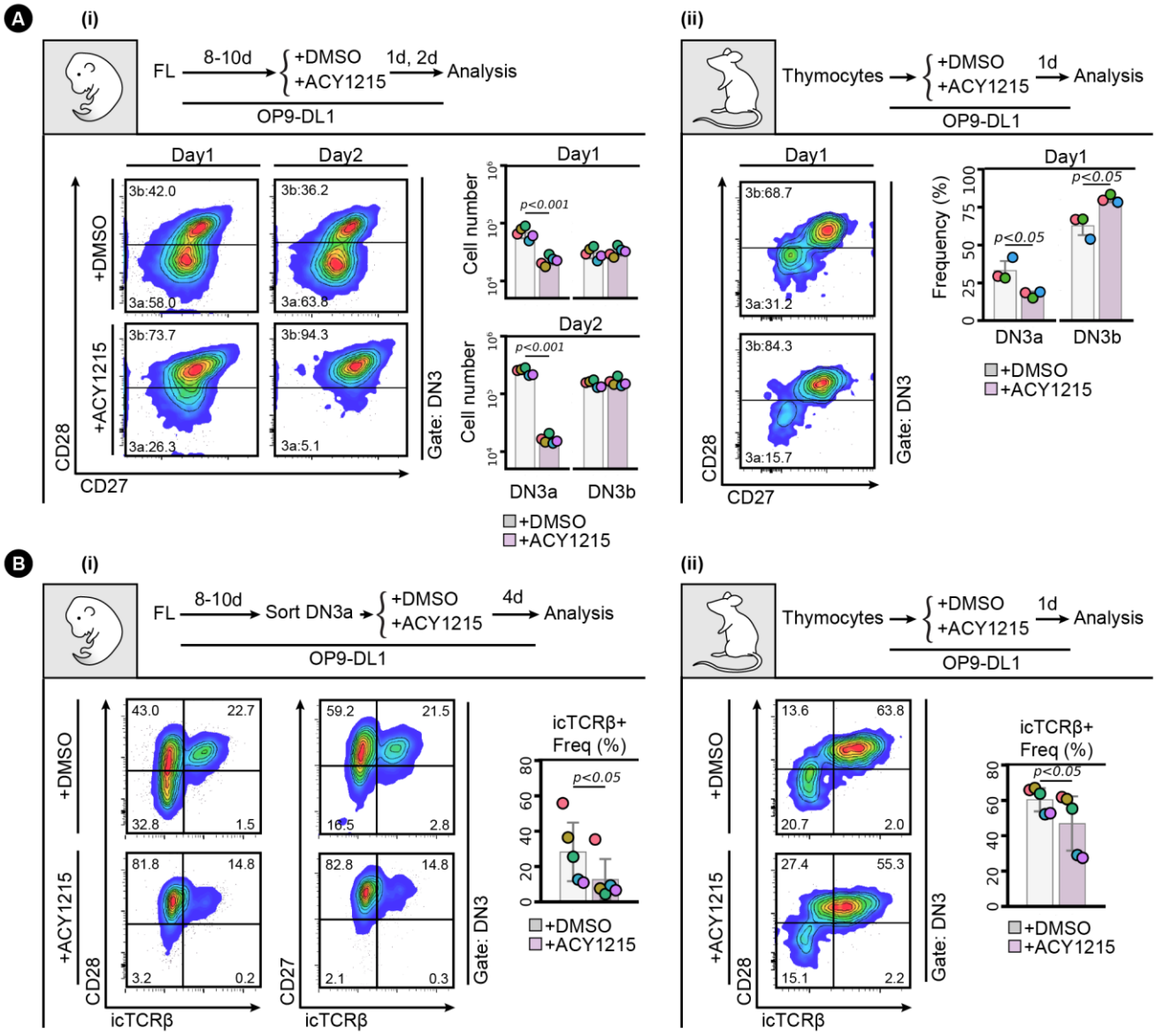
A
(i)
FL
8-10d
+DMSO
+ACY1215
1d, 2d
Analysis
OP9-DL1
Day1
Day2
3b:42.0
3a:58.0
3b:36.2
3a:63.8
3b:73.7
3a:26.3
3b:94.3
3a:5.1
+DMSO
+ACY1215
CD28
CD27
Gate: DN3
Cell number
p<0.001
DN3a
DN3b
(ii)
Thymocytes
1d
3b:68.7
3a:31.2
3b:84.3
3a:15.7
Frequency (%)
p<0.05
B
Sort DN3a
4d
43.0
22.7
32.8
1.5
81.8
14.8
3.2
0.2
59.2
21.5
16.5
2.8
82.8
14.8
2.1
0.3
icTCRβ
icTCRβ+
Freq (%)
13.6
63.8
20.7
2.0
27.4
55.3
15.1
2.2

Figure 3.

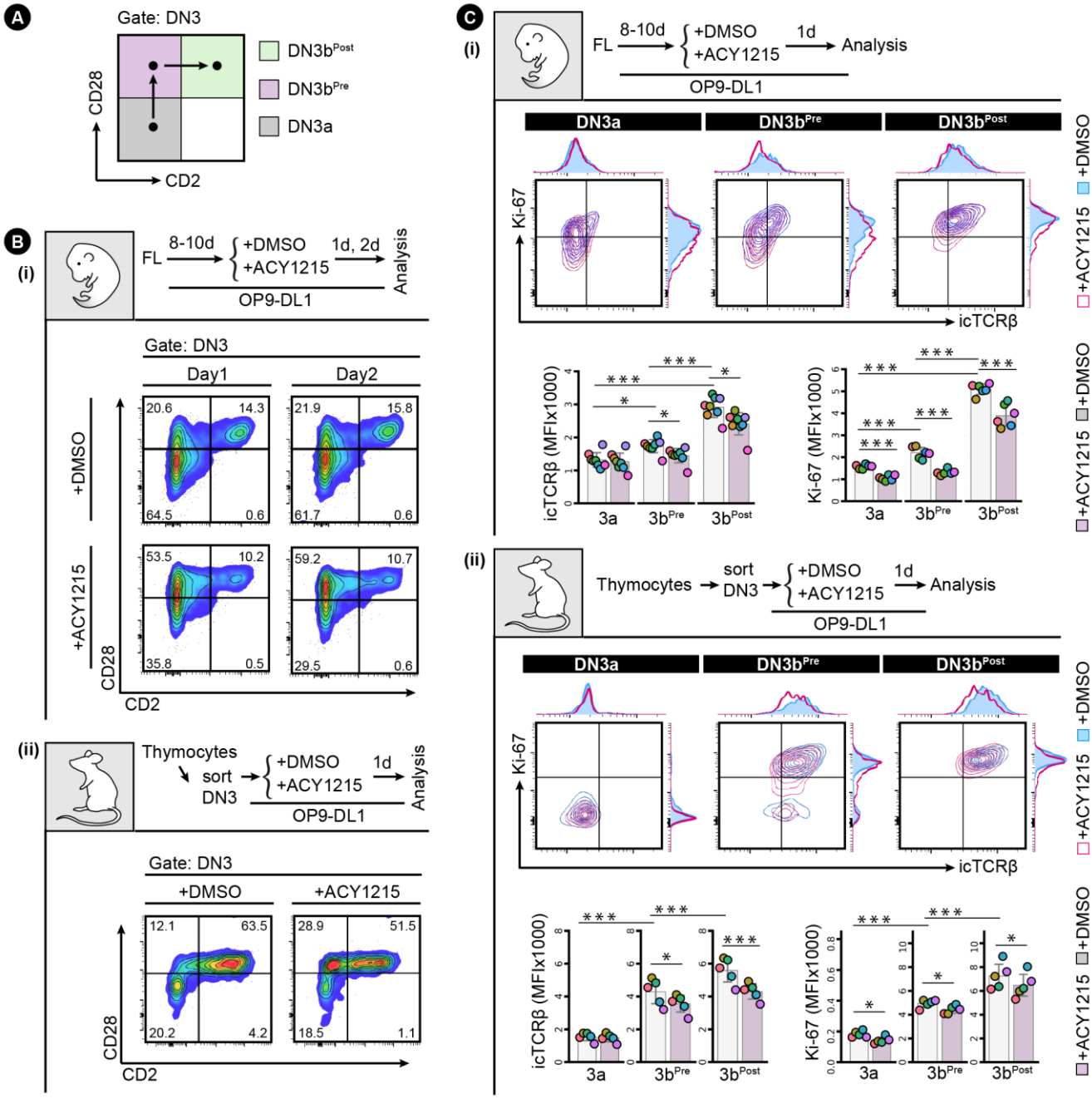

Chann et al. TCR co-receptors are expressed sequentially to fine-tune early αβ T cell development

Figure 4.

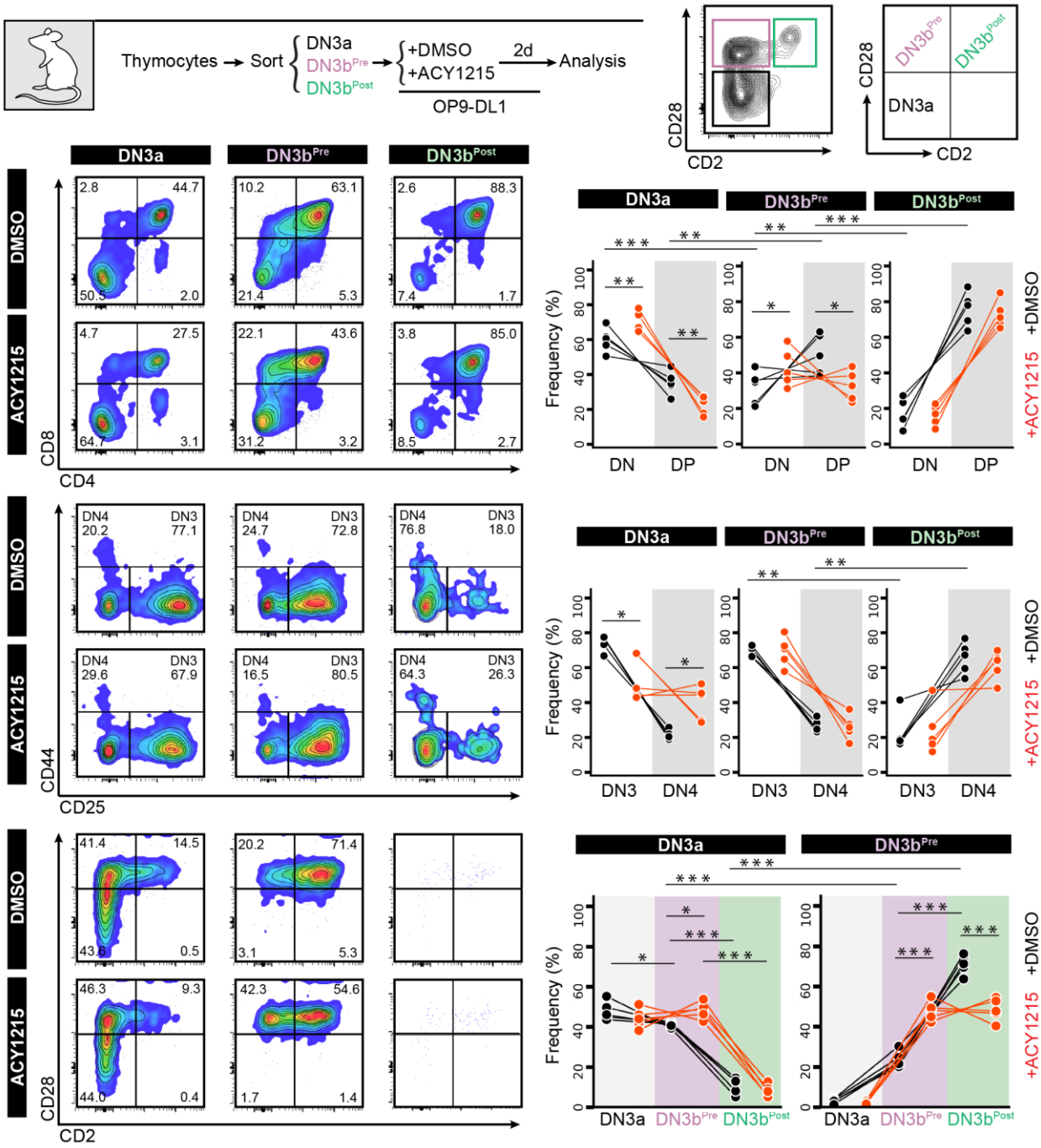
Thymocytes → Sort
DN3a
DN3b^Pre
DN3b^Post
+DMSO
+ACY1215
2d
Analysis
OP9-DL1
CD28
CD2
DN3b^Pre
DN3b^Post
DN3a
DMSO
ACY1215
CD8
CD4
CD44
CD25
Frequency (%)
DN
DP
DN3
DN4
+DMSO
+ACY1215

Figure 5.

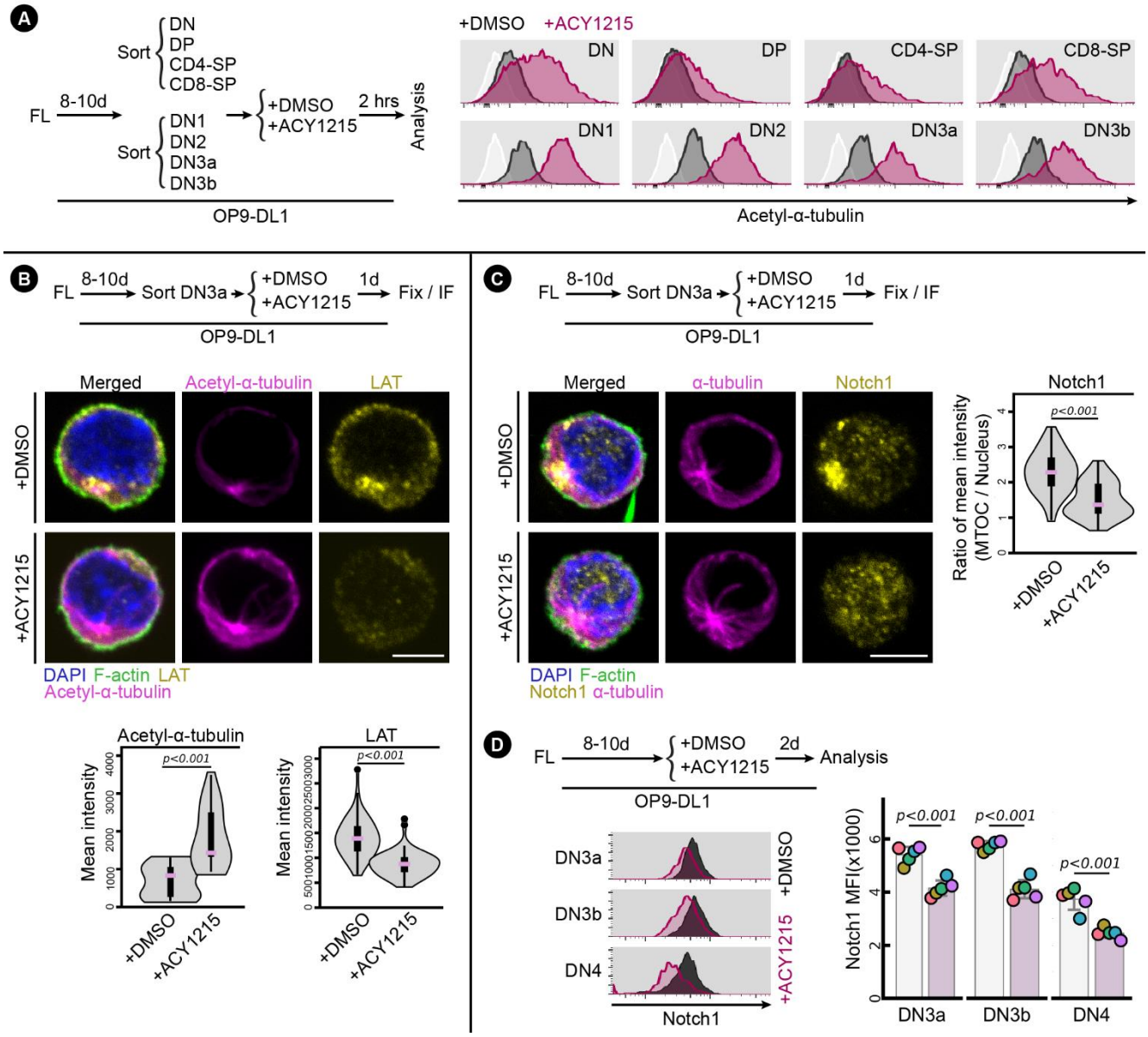
A
FL
8-10d
Sort
DN
DP
CD4-SP
CD8-SP
Sort
DN1
DN2
DN3a
DN3b
+DMSO
+ACY1215
2 hrs
Analysis
OP9-DL1
+DMSO
+ACY1215
DN
DP
CD4-SP
CD8-SP
DN1
DN2
DN3a
DN3b
Acetyl-α-tubulin
B
FL
8-10d
Sort DN3a
+DMSO
+ACY1215
1d
Fix / IF
OP9-DL1
Merged
Acetyl-α-tubulin
LAT
+DMSO
+ACY1215
DAPI F-actin LAT
Acetyl-α-tubulin
Acetyl-α-tubulin
Mean intensity
p<0.001
+DMSO
+ACY1215
LAT
Mean intensity
p<0.001
+DMSO
+ACY1215
C
FL
8-10d
Sort DN3a
+DMSO
+ACY1215
1d
Fix / IF
OP9-DL1
Merged
α-tubulin
Notch1
+DMSO
+ACY1215
DAPI F-actin
Notch1 α-tubulin
Notch1
Ratio of mean intensity
(MTOC / Nucleus)
p<0.001
+DMSO
+ACY1215
D
FL
8-10d
+DMSO
+ACY1215
2d
Analysis
OP9-DL1
DN3a
DN3b
DN4
+DMSO
+ACY1215
Notch1
Notch1 MFI(x1000)
p<0.001
p<0.001
p<0.001
DN3a
DN3b
DN4

Figure 6.

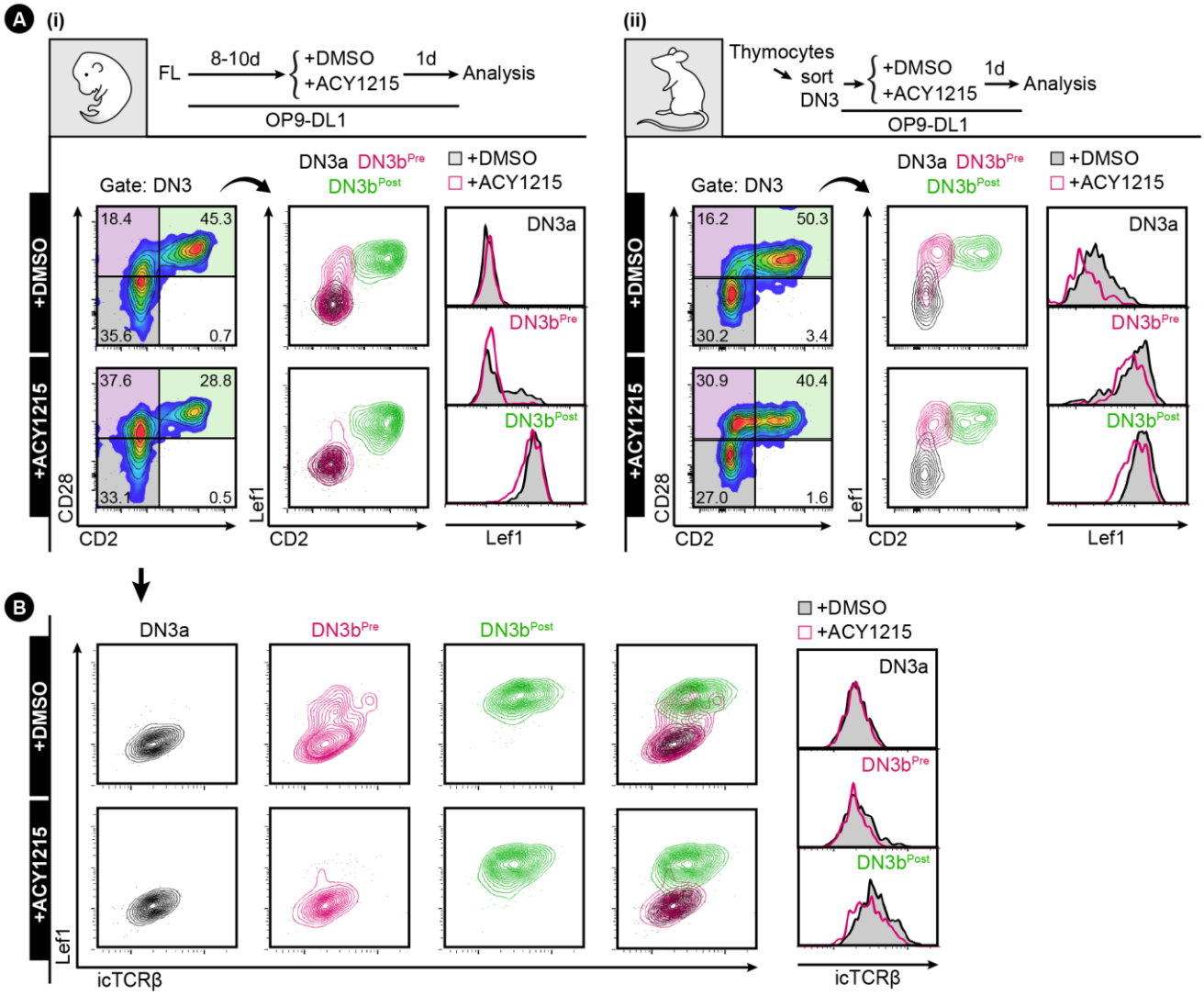
A
(i)
FL
8-10d
+DMSO
+ACY1215
1d
Analysis
OP9-DL1
Gate: DN3
DN3a
DN3b^Pre
DN3b^Post
+DMSO
+ACY1215
18.4
45.3
35.6
0.7
37.6
28.8
33.1
0.5
CD28
CD2
Lef1
(ii)
Thymocytes
sort
DN3
16.2
50.3
30.2
3.4
30.9
40.4
27.0
1.6
B
icTCRβ

Figure 7.

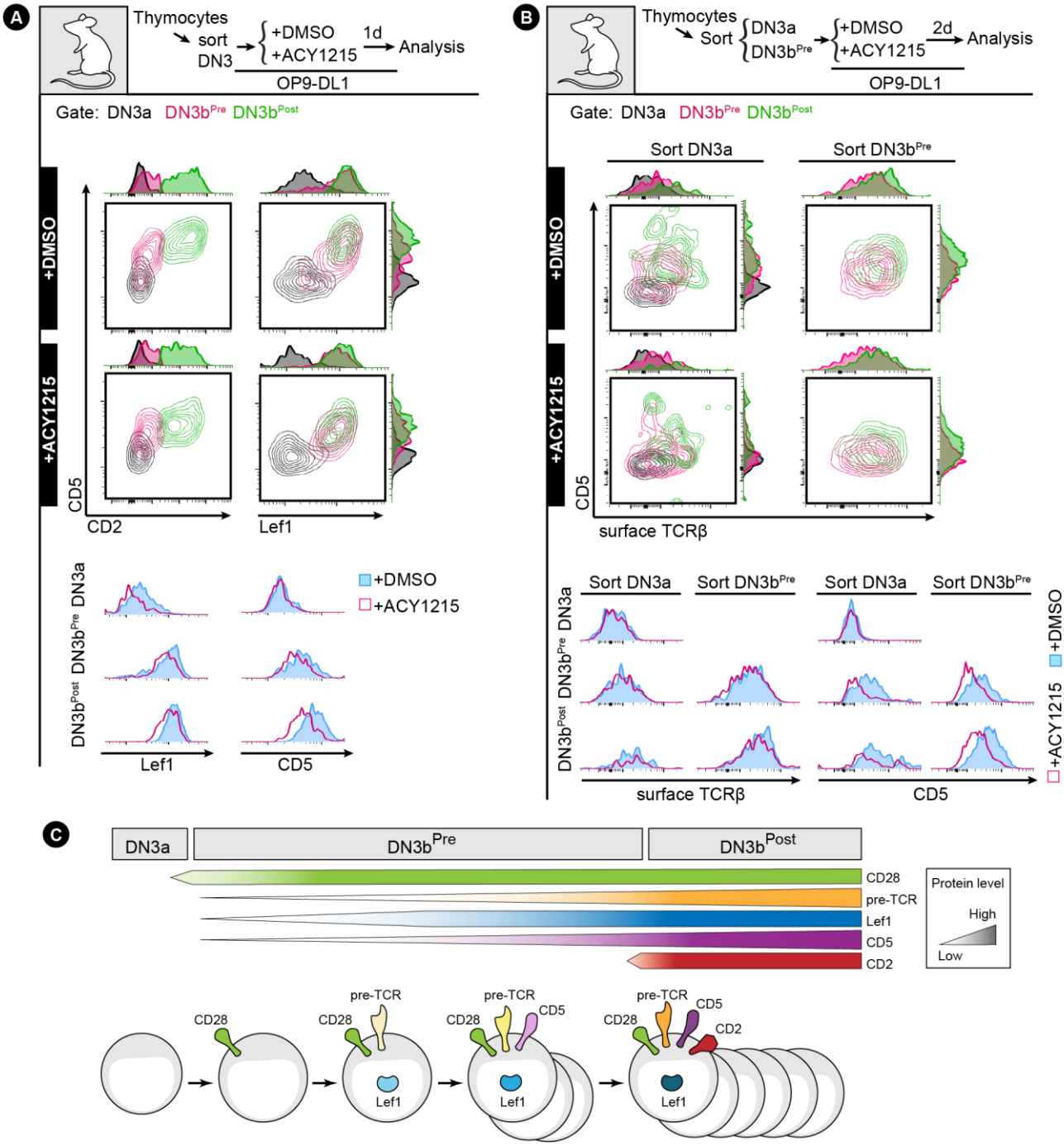

Chann et al. TCR co-receptors are expressed sequentially to fine-tune early αβ T cell development

Figure 8.

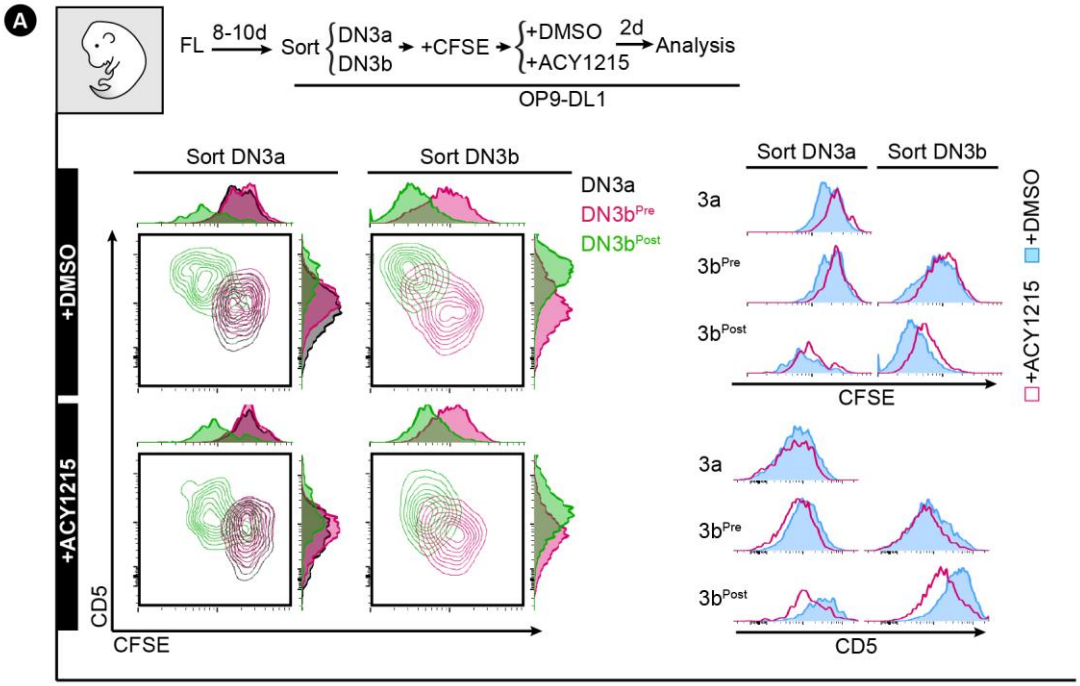
A
FL
8-10d
Sort
DN3a
DN3b
+CFSE
+DMSO
+ACY1215
2d
Analysis
OP9-DL1
Sort DN3a
Sort DN3b
DN3a
DN3b^Pre
DN3b^Post
+DMSO
+ACY1215
CD5
CFSE
3a
3b^Pre
3b^Post
CFSE
CD5
+DMSO
+ACY1215

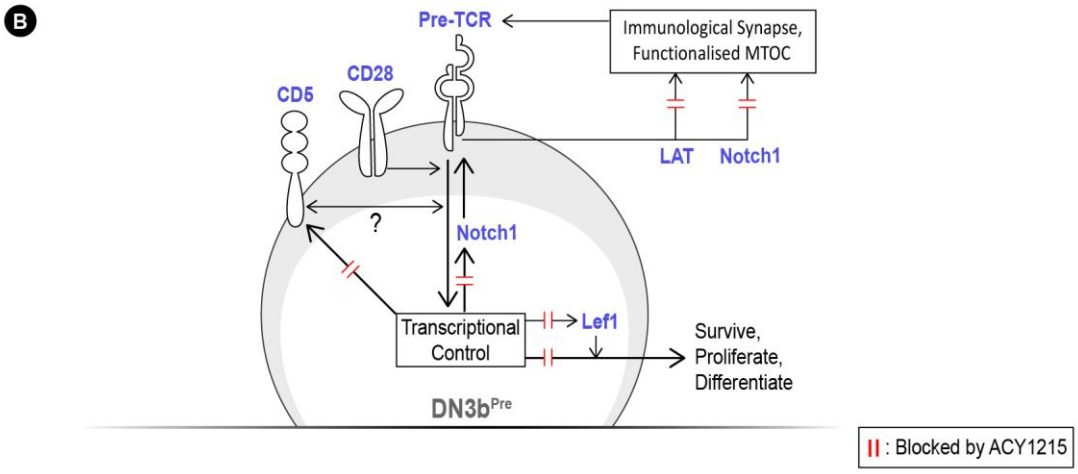
B
Pre-TCR
Immunological Synapse, Functionalised MTOC
CD28
CD5
LAT
Notch1
?
Notch1
Transcriptional Control
Lef1
Survive, Proliferate, Differentiate
DN3b^Pre
: Blocked by ACY1215

Supplementary Figure 1

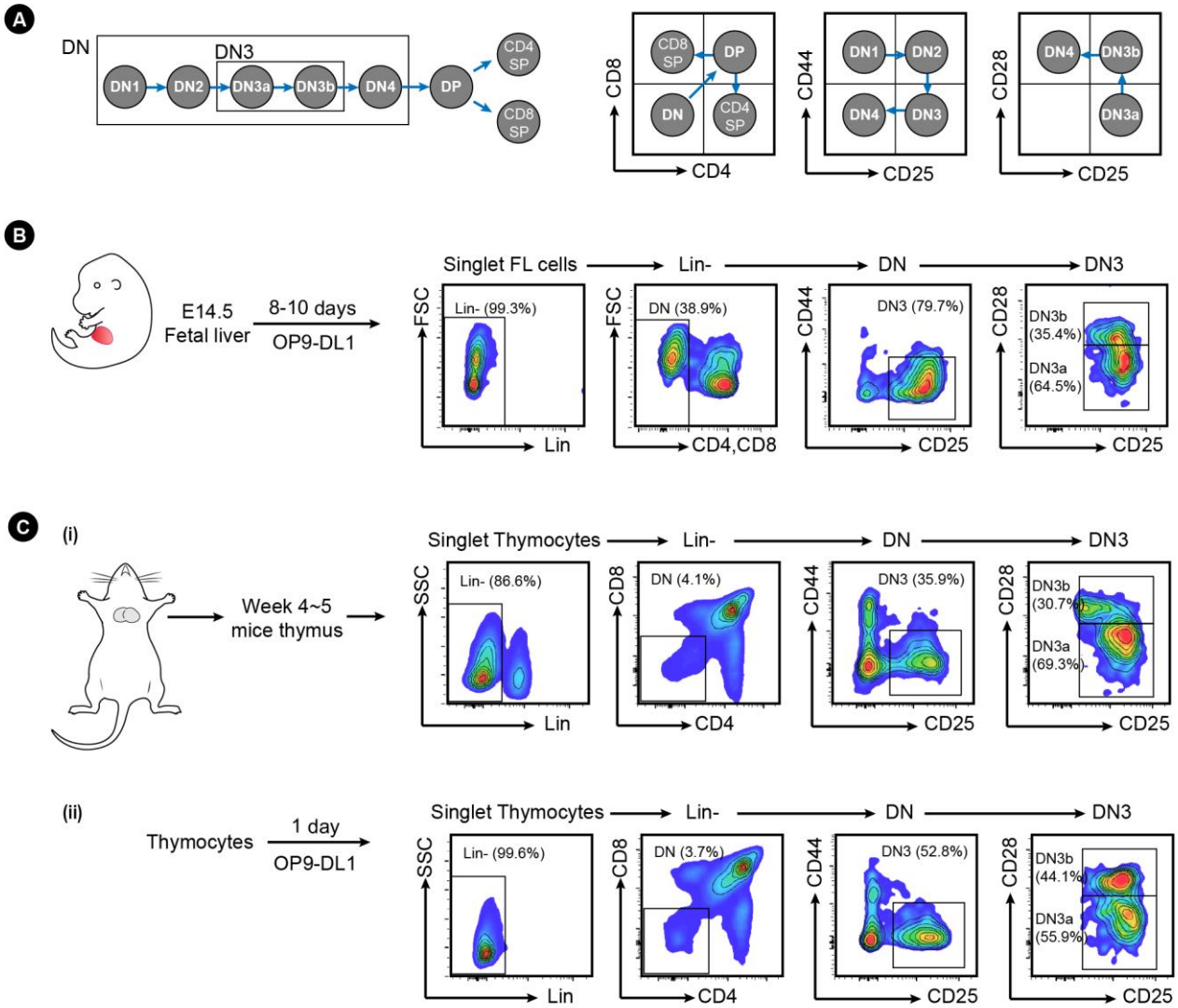

Supplementary Figure 2

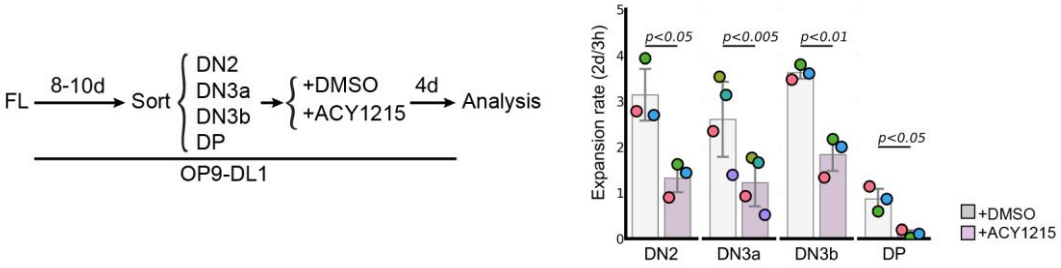

Supplementary Figure 3

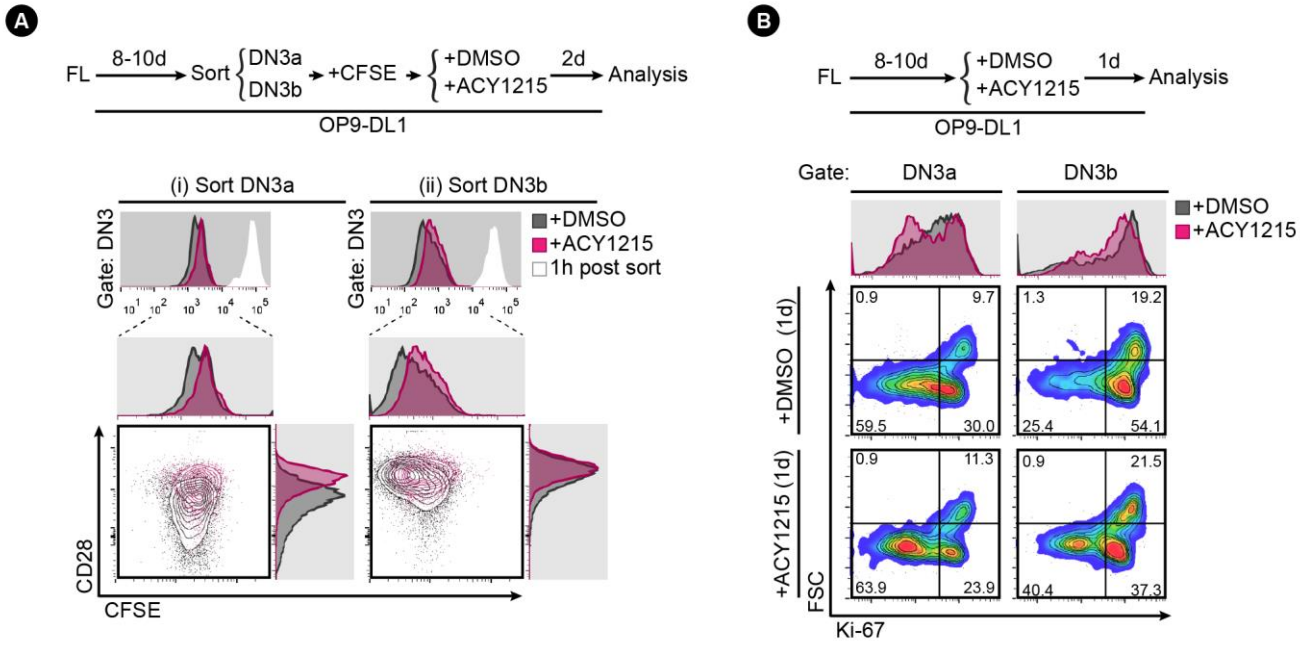

Supplementary Figure 4

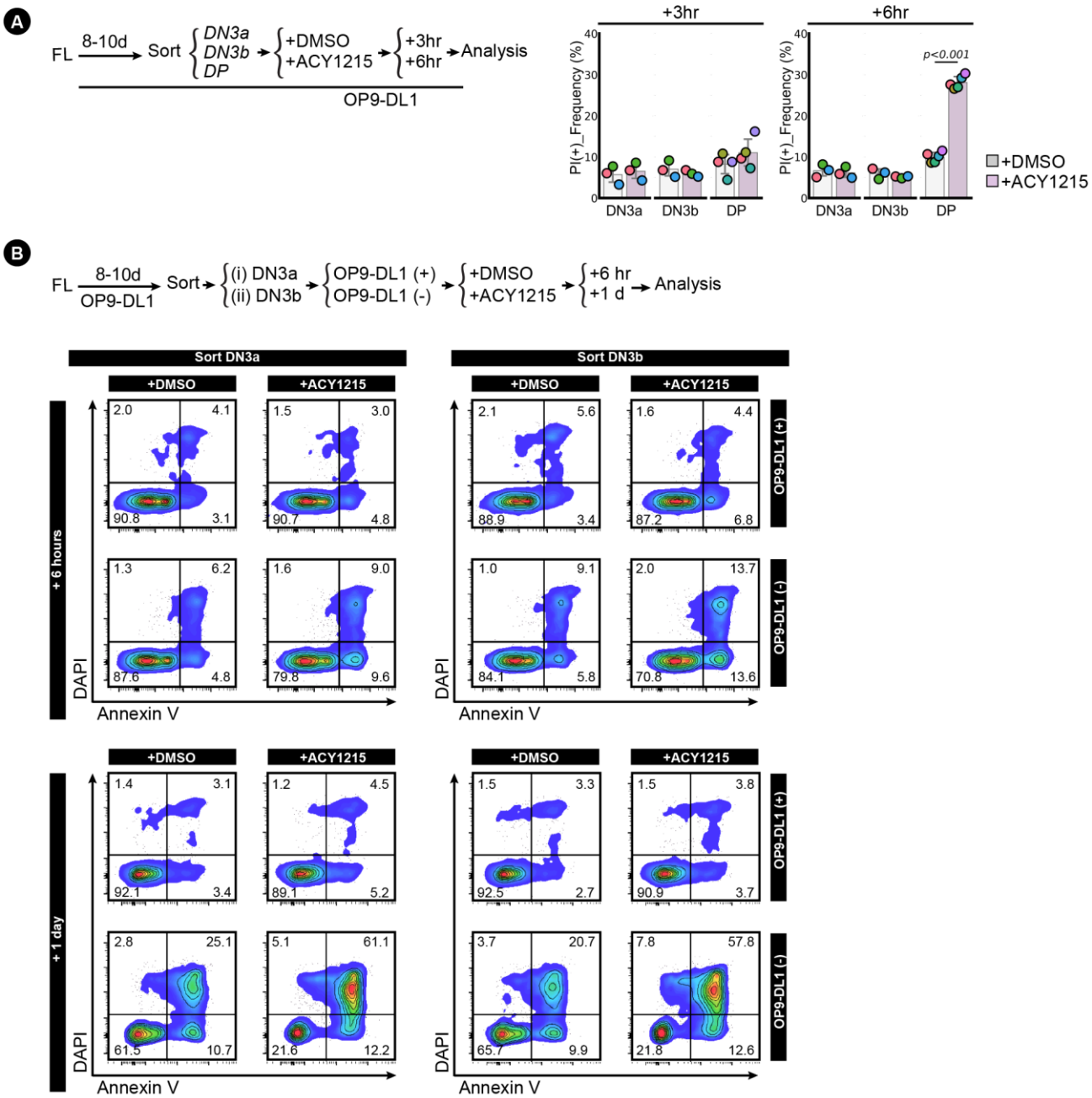

Supplementary Figure 5

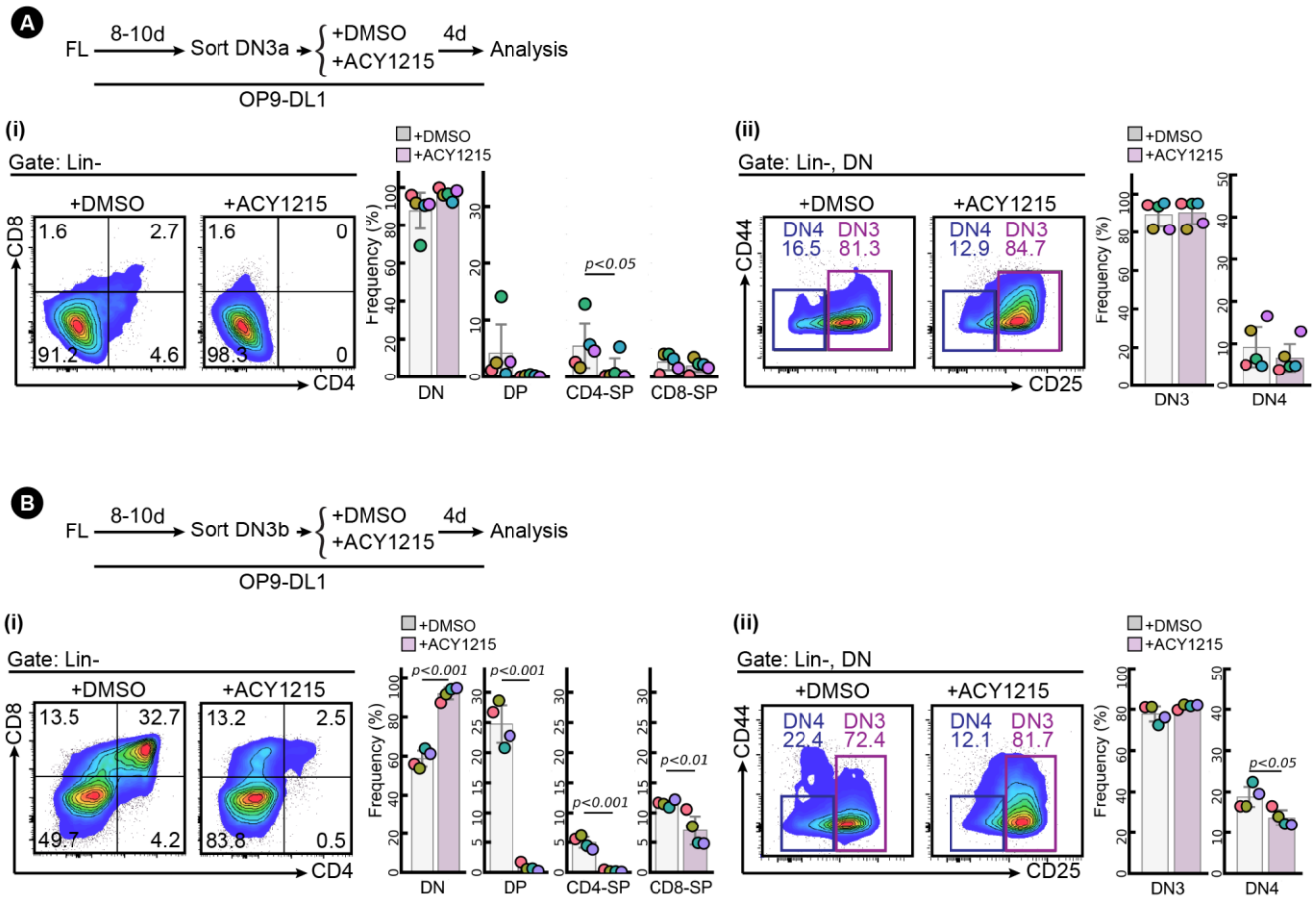

Supplementary Figure 6

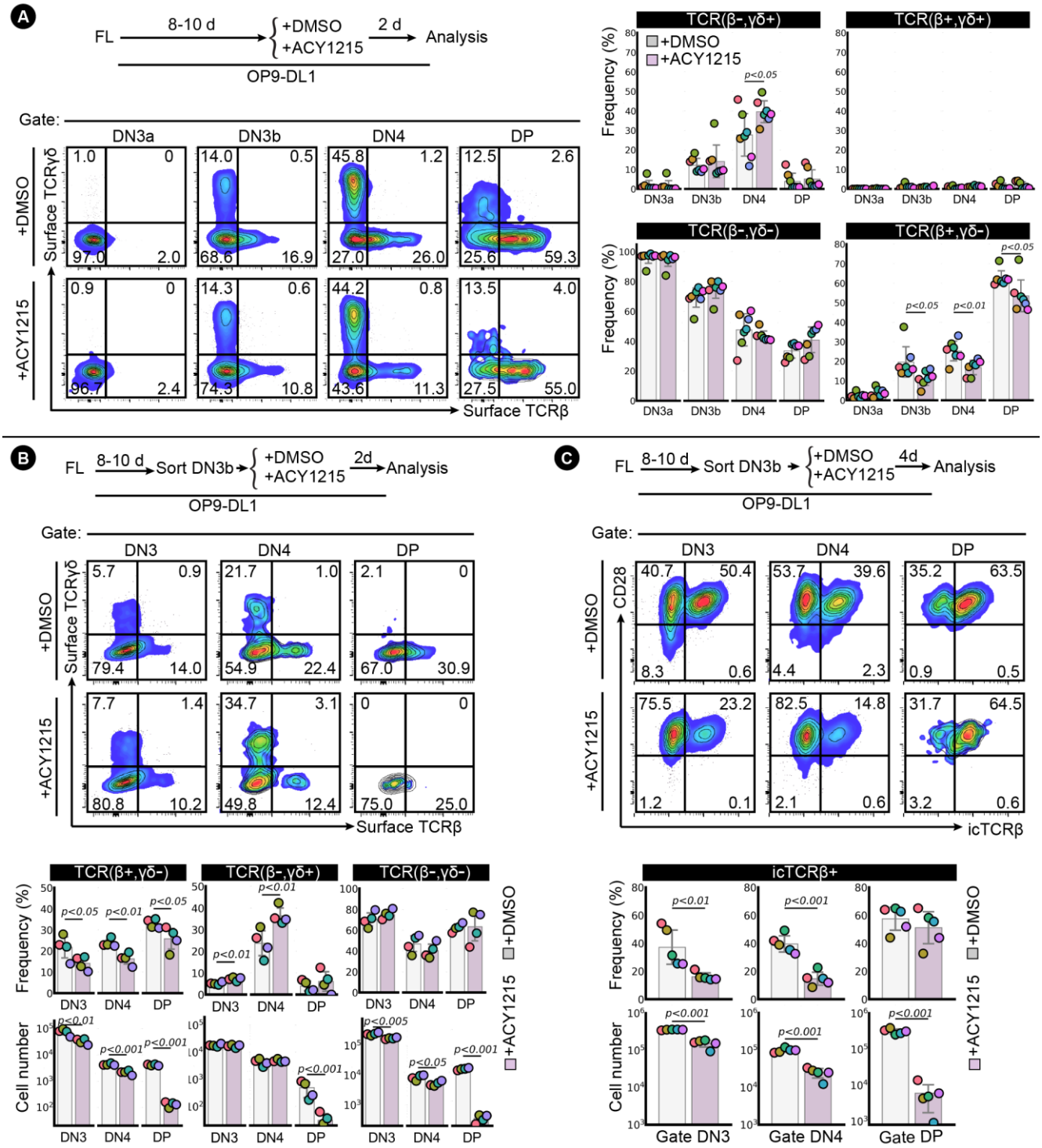

Supplementary Figure 7

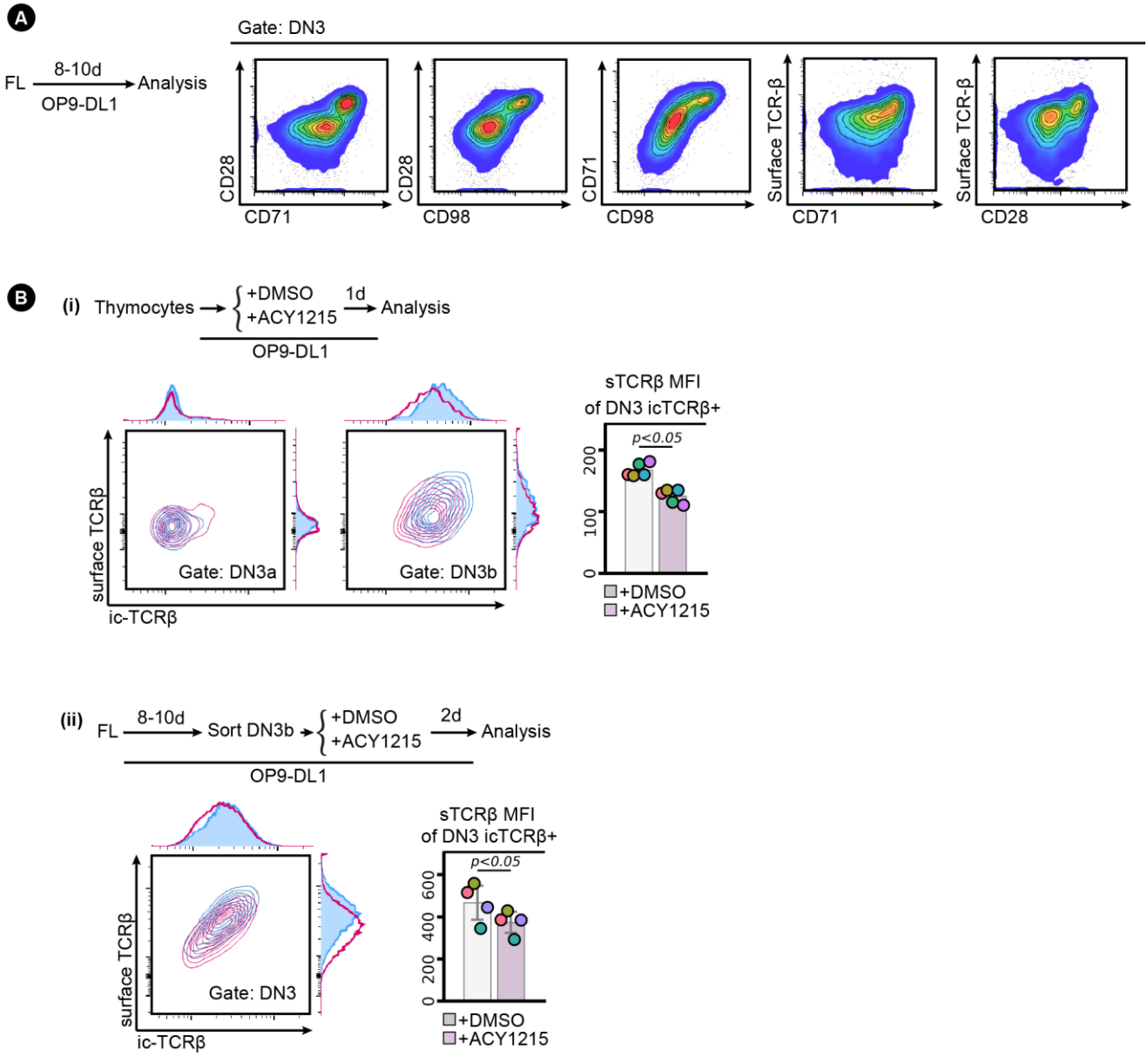

Supplementary Figure 8

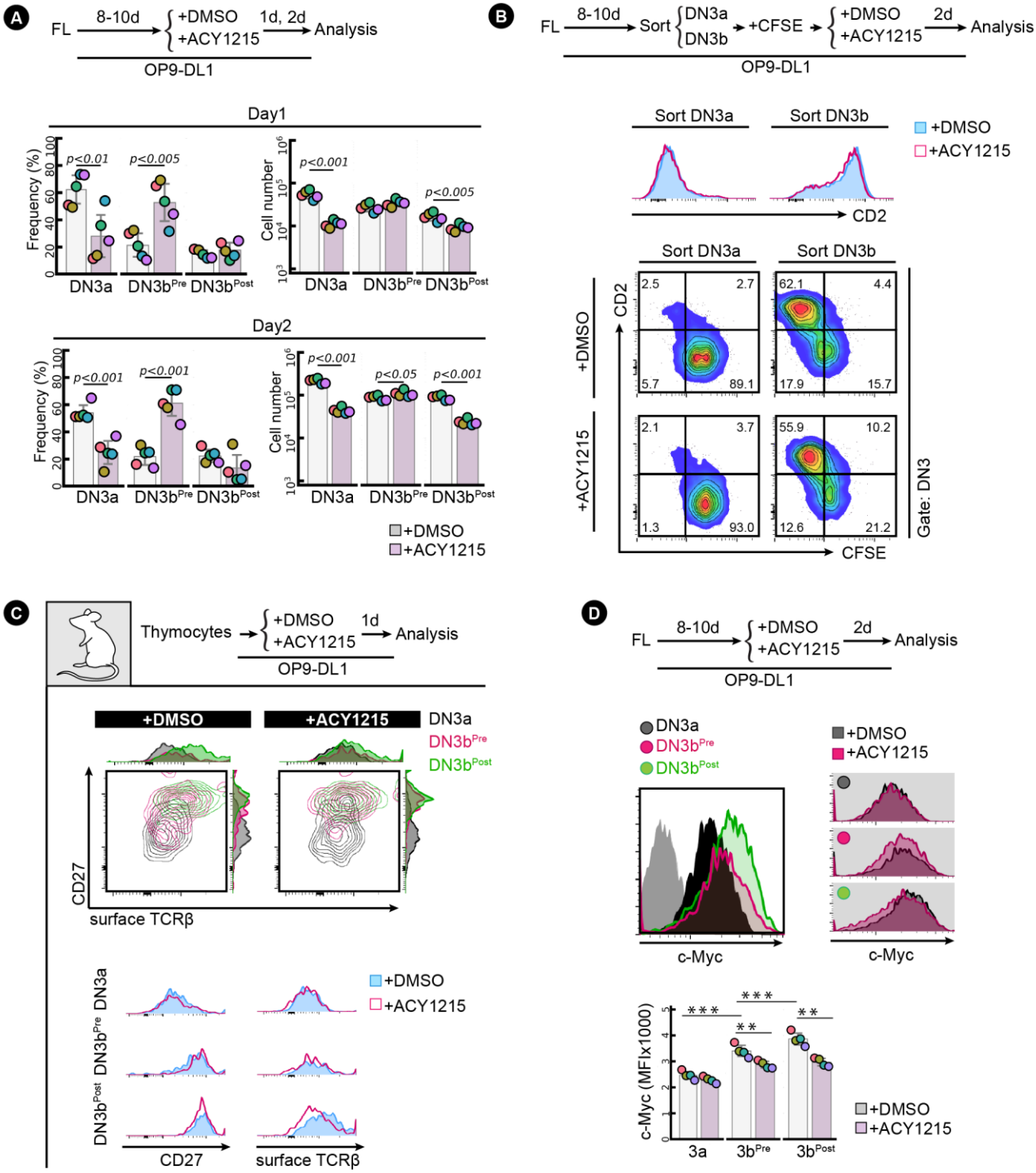

Supplementary Figure 9

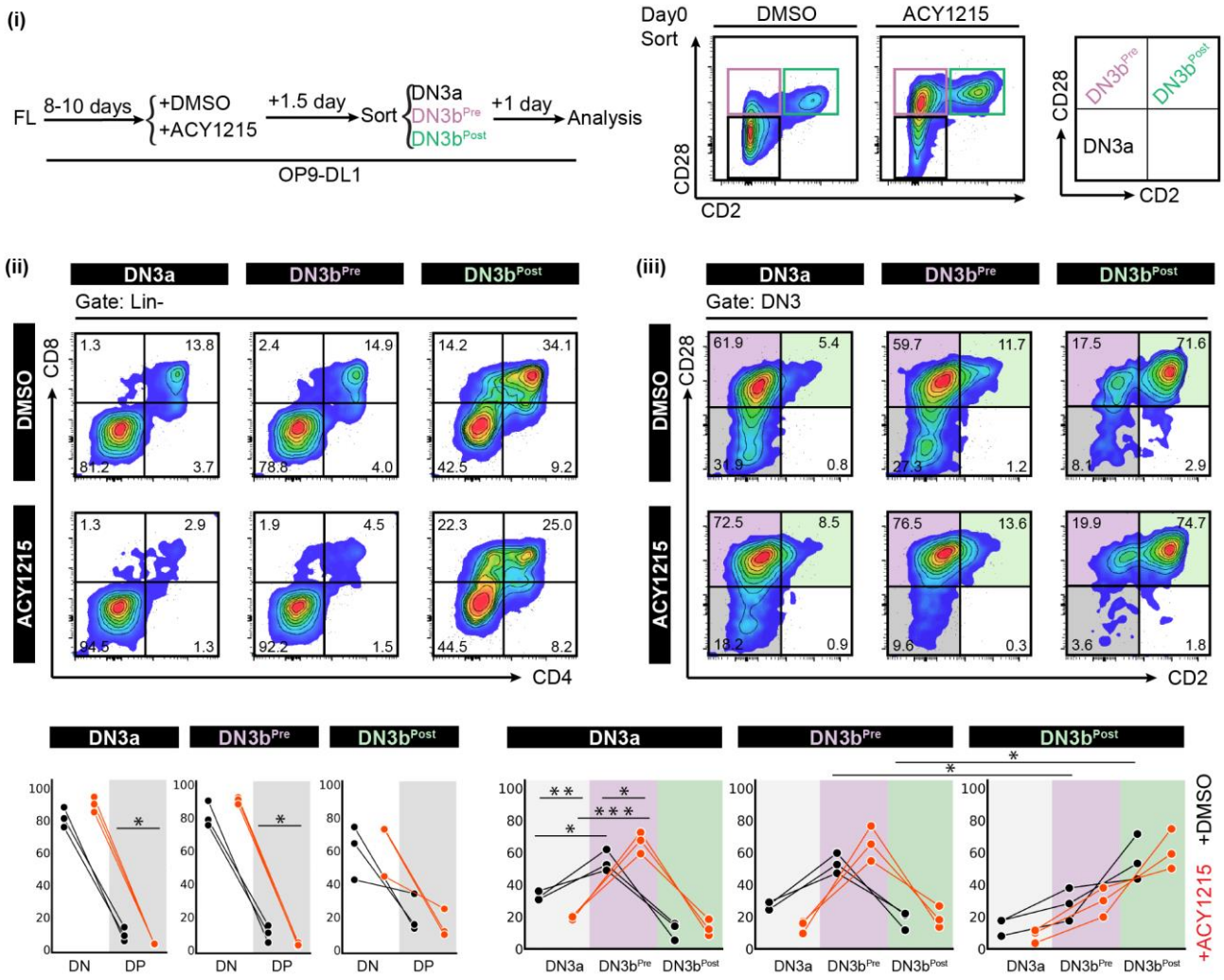

Supplementary Figure 10

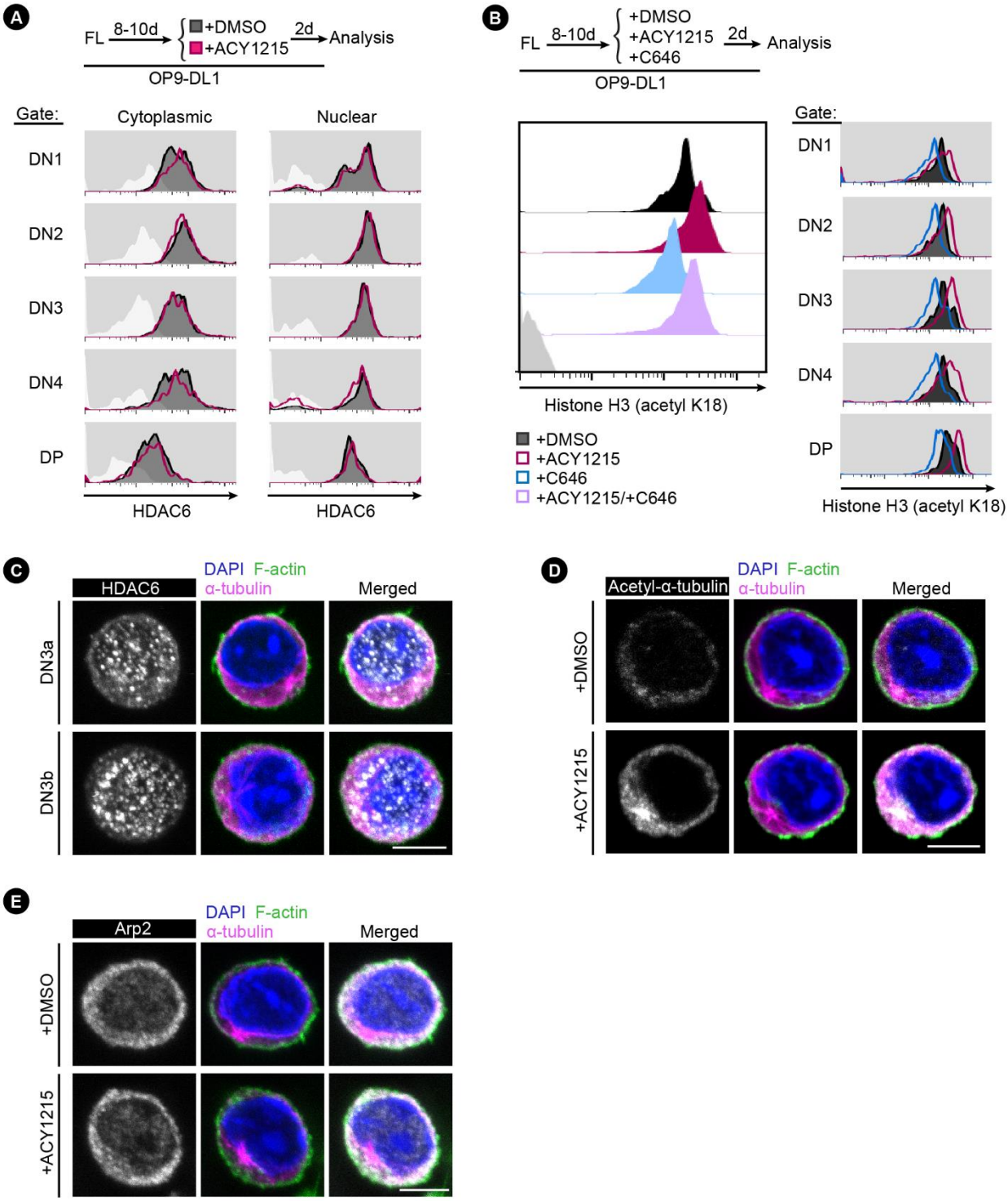

Supplementary Figure 11

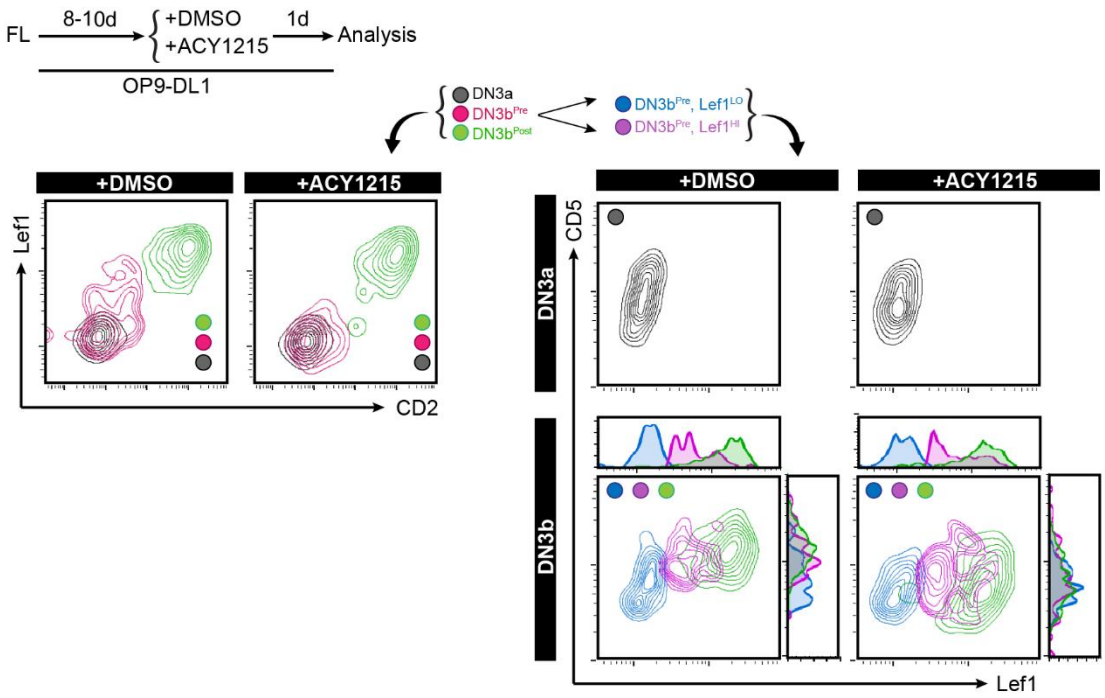

Supplementary Figure 12

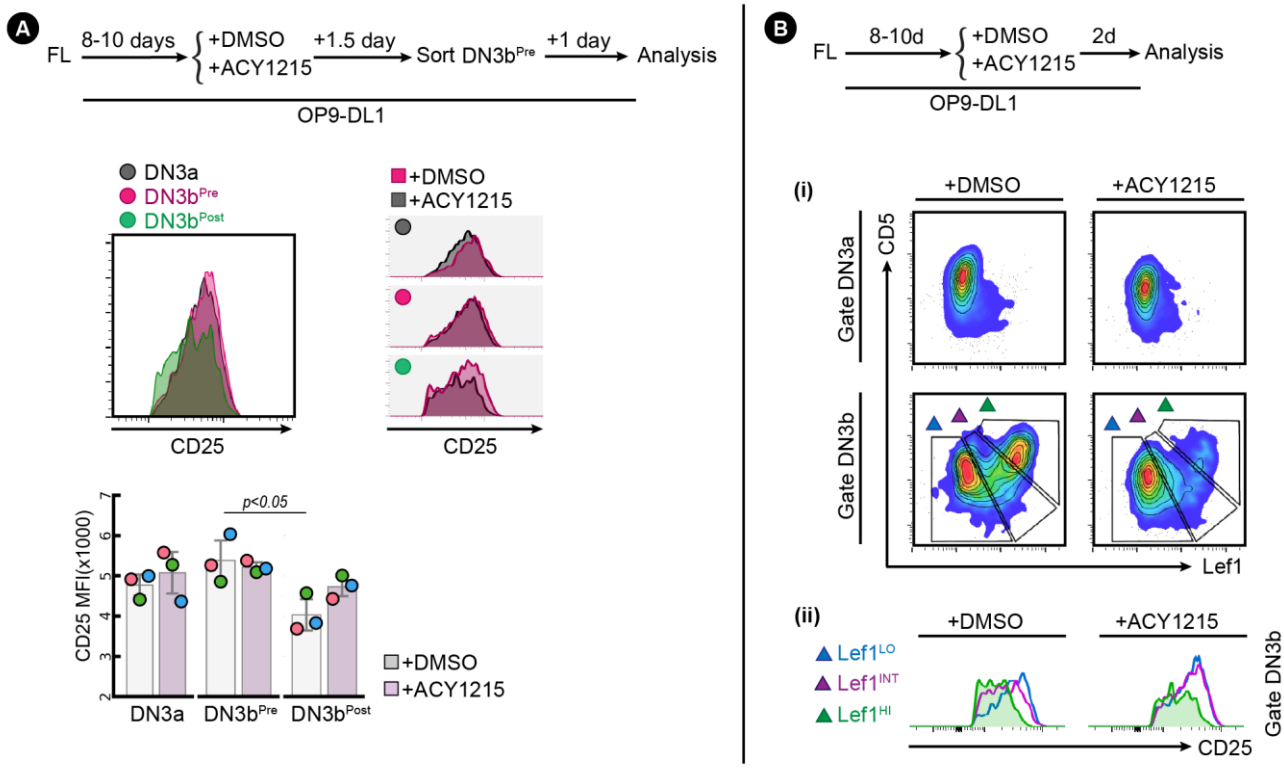

Supplementary Figure 13

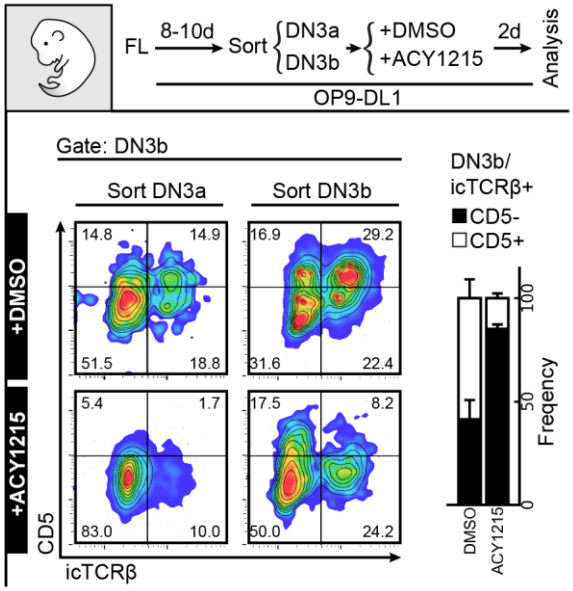

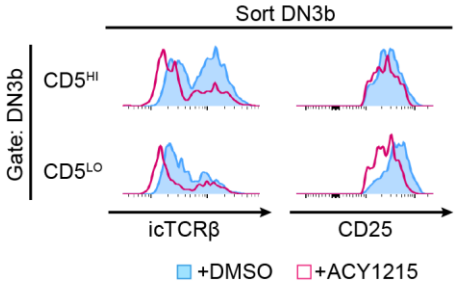
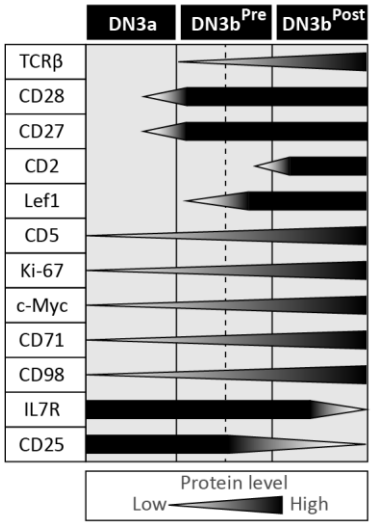
Supplementary Figure 14